

A Computational Method for Solving the Stochastic Joint Replenishment Problem in High Dimensions

Barış Ata

Booth School of Business, University of Chicago, Baris.Ata@chicagobooth.edu

Wouter J.E.C. van Eekelen

Booth School of Business, University of Chicago, Wouter.vanEekelen@chicagobooth.edu

Yuan Zhong

Booth School of Business, University of Chicago, Yuan.Zhong@chicagobooth.edu

November 18, 2025

We consider a discrete-time formulation for a class of high-dimensional stochastic joint replenishment problems. First, we approximate the problem by a continuous-time impulse control problem. Exploiting connections among the impulse control problem, backward stochastic differential equations (BSDEs) with jumps, and the stochastic target problem, we develop a novel, simulation-based computational method that relies on deep neural networks to solve the impulse control problem. Based on that solution, we propose an implementable inventory control policy for the original (discrete-time) stochastic joint replenishment problem, and test it against the best available benchmarks in a series of test problems. For the problems studied thus far, our method matches or beats the best benchmark we could find, and it is computationally feasible up to at least 50 dimensions—that is, 50 stock-keeping units (SKUs).

Key words: Inventory management, joint replenishment problem, economies of scale, impulse control, high-dimensional PDEs

1. Introduction

The joint replenishment problem (JRP) concerns the management of multi-item inventory systems, in which a fixed replenishment cost is incurred jointly by items procured together. A JRP is called stochastic (SJRP) when demands are random. A classical problem in operations management, the JRP has been extensively studied over several decades with wide-ranging applications; see, for example, the literature surveys in Goyal and Satir (1989), Aksoy and Erenguc (1988), Khouja and Goyal (2008) and Creemers and Boute (2022). In particular, the SJRP is relevant to sectors involving large-scale operations with highly variable demand and vast product assortments, such

as modern retail, where joint replenishment can amortize fixed costs such as transportation, and yield substantial economies of scale.

While coordinated replenishment offers attractive cost-saving opportunities, effective deployment in practice is challenging, especially when the number of distinct items, i.e., the problem dimension, is large. A fundamental reason is that item-level inventory decisions become interdependent under nonzero fixed replenishment costs. This interdependence creates two difficulties: (i) the computational effort required to solve the associated Markov decision process (MDP) scales with the sizes of the inventory state and decision spaces, both of which grow exponentially with dimension, leading to the “curse of dimensionality”; and (ii) fixed costs induce large multi-item orders, producing jumps in the inventory state and amplifying dimensionality effects. As a result, there has been limited progress in the literature on obtaining optimal replenishment policies in the multidimensional setting; see, for example, Section 6 of Perera and Sethi (2023b) for a review of related literature. Instead, a substantial body of literature has focused on designing effective heuristics for the SJRP; see, for example, Khouja and Goyal (2008). These heuristics typically propose intuitively appealing classes of parameterized inventory control policies, reducing the control problem to the optimization of the policy parameters.

In this paper, we revisit the classical SJRP (Goyal and Satir, 1989), which is formulated in discrete time, and develop an effective computational method for the high-dimensional setting. Toward this end, we consider a closely related continuous-time impulse control problem, in which instantaneous jumps in the system state can be effected at a fixed cost, and whose solution naturally leads to implementable policies for the original inventory control problem. Traditional numerical approaches to impulse control problems use grid-based methods, such as finite difference and finite element schemes, to solve the associated Hamilton-Jacobi-Bellman (HJB) partial differential equations (PDEs), but they also suffer from the curse of dimensionality. Compared to the discrete-time SJRP, the continuous-time impulse control formulation has a key advantage: It admits an equivalent probabilistic representation of the associated value function (Kharroubi et al., 2010). This representation allows us to employ the deep backward stochastic differential equation (BSDE) method developed in the seminal work of Han et al. (2018) for tackling high-dimensional problems. Since Han et al. (2018), a large literature has used deep neural networks to solve high-dimensional PDEs following the deep BSDE framework. We build on and contribute to this literature by de-

veloping a computational method for solving the high-dimensional impulse control problem. More importantly, we leverage that solution to propose effective control policies for the classical SJRP.

To put our method in perspective, we briefly review the deep BSDE framework, highlight our main challenges, and discuss the innovations we introduce to address them. Deep BSDE is a simulation-based computational approach for solving high-dimensional PDEs using deep neural networks. It starts from a probabilistic (BSDE) representation of the target function, typically a stochastic equality satisfied almost surely (a.s.) along sample paths of a *reference process*, which is a simulatable random process chosen by the algorithm designer. Based on this representation, one constructs a loss function and trains neural network approximations for the target function (and its gradient) by minimizing the loss, using samples generated by simulating the reference process. When the representation is a stochastic equality, the loss can be taken as the standard mean squared error between the left- and right-hand sides, with the function and gradient replaced by their neural network approximations, respectively. Under appropriate choices of the loss and the reference process, the success of the deep BSDE method then hinges primarily on extensive engineering efforts in hyperparameter tuning and neural network training.

For our impulse control problem, two immediate challenges arise in designing the loss and the reference process within the deep BSDE framework. First, while an equivalent probabilistic representation exists, it takes the form of a family of almost-sure stochastic inequalities rather than an equality (Kharroubi et al., 2010). To address this more complex case, we design a novel, non-standard loss that dualizes inequality constraints by incorporating a loss term for violations of the stochastic inequality and a tunable penalty parameter. The penalty parameter introduces considerable complications for neural network training, as its tuning schedule must be carefully coupled with the learning rate schedule to ensure training stability. Second, since the system state can be instantaneously displaced, deriving an effective control policy from the trained neural networks demands more than accurate local approximations of the value function and its gradient, as is common in prior literature (see, e.g., Han et al. (2018); Ata et al. (2024a); Ata and Kasikaralar (2023)); rather, the value function and its gradient must be well approximated across an expansive region of the state space. This, in turn, requires the reference process to explore the state space broadly. Indiscriminate exploration, however, yields irrelevant samples that hinder training. Thus, the reference process must strike an effective balance between exploration and exploitation; although this

trade-off has been considered in prior works, it is substantially more prominent and nuanced in the context of impulse control. Toward this end, we design several sophisticated reference processes with carefully designed state-dependent jumps to ensure that relevant samples are generated for efficient training.

As mentioned earlier, our neural network solution to the impulse control problem naturally yields implementable inventory control policies for the original (discrete-time) formulation of the SJRP. We demonstrate the effectiveness of these policies through a series of test problems in the original SJRP setting. For low-dimensional test problems, we compare our policies to the optimal ones derived by solving the MDPs associated with the original inventory control problem. For high-dimensional test problems, we benchmark our approach against the best available heuristic policies. In each low-dimensional case, our policy has an optimality gap of at most 1%. In the 36 high-dimensional test problems considered, our policy matches or beats the best available benchmark.

The rest of the paper is structured as follows. Section 2 provides an overview of related literature. Section 3 presents our model of the SJRP and its impulse control approximation. Section 4 introduces the HJB equation, and the aforementioned stochastic identity, Eq. (15). Section 5 describes our algorithm. Section 6 presents our test problems and the benchmark policies. Computational results are described in Section 7. We conclude in Section 8 with some discussion on possible future research directions. Appendices A–D contain further technical details, which include a formal derivation of the key stochastic identity, how the hyperparameters of our neural networks are tuned, a complete description of the benchmark policies, and the validation of our computational approach in a one-dimensional inventory model with fixed cost.

2. Literature Review

We review the following three relevant streams of literature: (i) joint replenishment problems, (ii) impulse control problems, and (iii) deep learning methods for solving high-dimensional PDEs.

Joint replenishment problems. The JRP is a classical problem in inventory management that has received considerable research attention over the past few decades. Broadly speaking, the JRP literature can be divided into problems with deterministic demand and those with stochastic demand (Goyal and Satir, 1989). The deterministic JRP can be viewed as the most basic multi-item extension of the classical economic order quantity (EOQ) model (Harris, 1990). It assumes constant demand rates over an infinite planning horizon, with replenishment occurring at regular

intervals. The objective is to determine the optimal frequency for replenishing the different items (see, e.g., Viswanathan, 1996; Kaspi and Rosenblatt, 1991; Goyal and Belton, 1979). One class of effective policies is characterized by the power-of-two rule under which orders are placed at power-of-two multiples of a base period. Roundy, 1985, 1986; Jackson et al., 1985 have shown that the best power-of-two policies can perform within two to six percent of optimality. Much of the (deterministic) JRP literature focuses on the following cost structure: there is a group replenishment fixed cost, which is incurred every time an order is placed, and there are individual fixed costs for each item. By contrast, the generalized JRP (GJRP) allows the shared fixed costs to depend on the given collection of items included in the replenishment (Federgruen and Zheng, 1992). Adelman and Klabjan (2005) prove the existence of optimal policies for the GJRP with capacity constraints using duality theory. Adelman and Klabjan (2012) use approximate dynamic programming to determine near-optimal policies in this setting.

Our paper, however, concerns the SJRP; we now review this literature. For the single-item problem with procurement fixed costs, Scarf (1960) shows that the optimal policy has the following simple structure: If the inventory level drops to or below a fixed level s , an order is placed to raise it back to another fixed level S . Efficient algorithms exist to find optimal parameters for such (s, S) policies; see, for example, Veinott Jr and Wagner (1965); Zheng and Federgruen (1991). Since Scarf's seminal work, there have been several attempts to identify effective structural properties of optimal policies for multi-item inventory models. We refer the readers to Perera and Sethi (2023a) for a detailed review of these works, and discuss only the most relevant literature. Johnson (1967) considers an infinite-horizon, d -item SJRP in discrete time, with integer-valued demand and the inventory process living in the state space \mathbb{Z}^d . The demand in each time period is allowed to depend on the initial inventory levels in that period. The cost structure is identical to ours, i.e., there is a single fixed cost and linear, item-specific variable costs, whenever an order is placed. He considers both the total discounted cost and long-run average cost objectives and establishes the optimality of a so-called (σ, S) policy under both objectives, where σ is a subset of \mathbb{Z}^d , and S is a vector in \mathbb{Z}^d . Under this policy, if the inventory state x is in σ and $x \leq S$ component-wise, then one orders up to the levels S , and does not order if $x \notin \sigma$. Note that the policy is not specified when $x \in \sigma$ and $x \not\leq S$, but if the initial inventory state $x \leq S$, then under a (σ, S) policy, the inventory state always stays below S (component-wise), so a (σ, S) policy is optimal in

this case. Furthermore, for the long-run average cost objective, even if the initial state $x \not\leq S$, an optimal policy can simply first wait for the inventory levels to deplete and drop below S , and then follow a (σ, S) policy. Kalin (1980) proves the optimality of (σ, S) policies under conditions that are different from those in Johnson (1967), and characterizes the complement of σ , a set where no order is placed, as being increasing under a certain partial ordering. His proof makes use of the notion of (K, η) -quasiconvexity in \mathbb{R} , a generalization of the concept of quasiconvexity used in Porteus (1971) and in Schäl (1976), for various single-item inventory problems. Gallego and Sethi (2005) recovered results in Kalin (1980) using generalized notions of K -convexity in \mathbb{R}^d , a concept originally introduced in Scarf (1960). Even though the optimal policy structure is known when the initial inventory state $x \leq S$, determining the ordering region σ and the order-up-to level vector S is extremely challenging computationally, especially in high dimensions.

Due to the computational intractability, research on SJRP often focuses on classes of parameterized control policies that are intuitively appealing. Once attention is restricted to a particular class of control policies, the problem reduces to optimizing the policy parameters. This is often accomplished by numerical evaluations of the policy performances through simulation. See, for example, Atkins and Iyogun (1988); Federgruen et al. (1984); Ignall (1969); Silver (1965, 1981); Viswanathan (1997); Balintfy (1964). For a comprehensive review of the various heuristic control policies, we refer to Khouja and Goyal (2008).

Impulse control problems. One year after Scarf established the optimality of the (s, S) policy in discrete time, Beckmann (1961) demonstrates that this policy is also optimal in continuous time with Poisson demand. To prove this, Beckmann (1961) uses what is known as uniformization. This approach restricts ordering decisions to occur only at the jumps of the Poissonian demand, effectively reducing the problem to its discrete-time counterpart. To address more general demand models such as diffusion or mixed-diffusion processes, impulse control problems offer a flexible framework that can effectively capture the lump-sum ordering nature of continuous-time inventory control problems with fixed costs. These stochastic control problems allow the system controller to intervene through jumps in the underlying state space (Bensoussan and Lions, 1984). Several authors have used the associated HJB equations to prove the optimality of (s, S) -type policies for various one-dimensional inventory models; see, for example, Constantinides (1976); Harrison et al. (1983); Sulem (1986); Bensoussan et al. (2005); Helmes et al.

(2017). For applications of the one-dimensional impulse control problems in economics, we refer the reader to Stokey (2008).

While numerous studies have investigated the continuous-time inventory model with fixed costs for single-item problems, only a handful of paper have addressed multi-item problems (Perera and Sethi (2023a)). A pioneering attempt to solve the multi-item setting is made by Sulem (1986), who considers a two-item inventory system with constant, deterministic demand rates. There are individual fixed costs for ordering a single item, and a fixed cost of ordering both items, which is lower than the sum of individual fixed costs. The variable costs are assumed to be zero. Using the associated HJB equation, she establishes the optimality of a (γ, Γ) policy, where γ represents the ordering boundary, and Γ denotes the order-up-to level boundary, similar to the (σ, S) policy in the discrete-time setting. Li and Sethi (2022) also consider two-item inventory systems, and extend Sulem (1986) in several ways. First, they allow variable costs, and establish the optimality of a (γ, Γ) policy in the deterministic setting with constant demand rates. They provide characterizations of the boundaries γ and Γ in this case, facilitating their numerical constructions. Second, they establish various theoretical properties of a stochastic model with diffusion demand, such as the (K, η) -quasiconvexity of the value function, and used the finite-difference scheme to obtain numerical solutions. Their numerical study suggests that the optimal policy in the stochastic case is also of the (γ, Γ) type. Note that their finite-difference scheme is not computationally feasible in high-dimensional settings, i.e., when the number of distinct items is large. Other common numerical methods for solving impulse control problems include iterated optimal stopping and policy iteration; see, e.g., Azimzadeh et al. (2018), Azimzadeh and Forsyth (2016), and Chapter 12 in Øksendal and Sulem (2019). Unfortunately, these methods face the same computational tractability issues.

Deep learning methods for solving high-dimensional PDEs. Deep learning has gained significant traction as a method for solving high-dimensional PDEs since the seminal papers E et al. (2017); Han et al. (2018). Their method uses the probabilistic characterization of semilinear PDEs as backward stochastic differential equations (BSDEs); see, for example, (Yong and Zhou, 1999, Chapter 7). The method outlined in Han et al. (2018) proposes to discretize the BSDE forward in time using a standard Euler scheme, and approximate the value function and its gradient with neural networks. It then learns the value function and its gradient by optimizing the neural network

parameters through minimization of the expected squared distance between the known terminal value and the discretized BSDE’s terminal value. We refer to Han and Long (2020) for a detailed convergence study. With the advent of high-performance GPU computing, these deep-learning methods have been successfully applied to solve high-dimensional PDEs; see Beck et al. (2022); E et al. (2021); Chessari et al. (2023) for extensive literature reviews on the subject.

Ata and Kasikaralar (2023) and Ata et al. (2024b,a) introduced these techniques to the operations management domain. The former studies a semilinear parabolic PDE linked to a drift control problem arising in dynamic call center scheduling, while the latter two develop computational methods for solving control problems in stochastic processing networks in the heavy-traffic regime. Ata and Zhou (2024) solves a sequential vehicle routing problem motivated by an eviction enforcement application using a similar approach. Ata et al. (2024c) studies dynamic control of a make-to-order manufacturing system with throughput time constraints in high dimensions using deep learning. Ata and Xu (2025) solves a high-dimensional dynamic stochastic matching problem building on the deep BSDE method. Our approach draws extensively from the foregoing literature; however, to the best of our knowledge, none of the existing methods can handle impulse control. Our novel deep-learning framework is inspired in part by the mathematical finance literature (Buehler et al., 2019; Biagini et al., 2023), where deep learning is employed to identify optimal hedging strategies for pricing financial derivatives, problems often modeled by nonlinear PDEs. Indeed, as mentioned earlier, our approach relies on a stochastic identity (Eq. (15)) that exploits a connection between impulse control problems and the so-called stochastic target problems, the latter of which have been studied extensively in the mathematical finance literature (see, e.g., Touzi, 2012, Chapter 7). Finally, Bayraktar et al. (2023) studies an optimal switching problem – which is closely related to impulse control problems (Bouchard (2009)) – with applications to energy markets, building on the framework developed in Huré et al. (2020).

3. Model

Consider a warehouse that stocks and sells d different items. The warehouse manager may place orders for any subset of these items. Define the order vector $y = (y_1, \dots, y_d)^\top$, where $y_i \geq 0$ denotes the number of units of item i ordered and the superscript \top denotes transpose, and let $c(y)$ denote

the total ordering cost, where

$$c(y) = \begin{cases} c_0 + \sum_{i=1}^d c_i y_i, & \text{if } \sum_{i=1}^d y_i > 0, \\ 0, & \text{otherwise.} \end{cases}$$

That is, the warehouse manager incurs a fixed cost c_0 for placing the order—for example, c_0 may represent the fixed cost of using a shared resource associated with an order such as the transportation cost incurred from using a truck—and $c_i y_i$ denotes the associated variable cost of ordering y_i units of item i for $i = 1, \dots, d$.

We let $x = (x_1, \dots, x_d)^\top$ denote a generic system state, where x_i represents the inventory level of item i . The warehouse manager reviews the system state periodically at times $n = 1, 2, \dots$. At the beginning of each period, upon observing the system state, but before observing demand, he makes an ordering decision; it is possible that the manager decides not to place an order. If an order is placed, it is received immediately, i.e., the delivery lead time is zero. Then, at the end of the time period, demand is realized, and any unmet demand is backlogged. In addition to ordering costs, there are linear holding and backlog costs. To be specific, a penalty cost p_i is incurred for each unit of backlogged demand of item i , and a holding cost h_i is charged for each unit of inventory of item i carried over from one period to the next. Thus, if we let

$$f_i(x_i) = \begin{cases} h_i x_i, & x_i \geq 0, \\ -p_i x_i, & x_i < 0, \end{cases} \quad (1)$$

then we have that

$$f(x) = \sum_{i=1}^d f_i(x_i)$$

is the per-period state cost born by the system manager when the system state is x . All costs are incurred at the end of the period.

We now describe the system dynamics mathematically. First, let $X(n)$ denote the system state (i.e., the vector of inventory levels for items $1, \dots, d$) at the end of period n . Second, let $\xi(n)$ denote the d -dimensional demand vector in period n . To facilitate future analysis, we define the cumulative demand until period n as

$$D(n) = \sum_{k=1}^n \xi(k), \quad n \geq 1. \quad (2)$$

Third, let $y(n) \geq 0$ denote the order vector in period n . Then, the evolution of the system state can be expressed as

$$X(n) = X(n-1) + y(n) - \xi(n), \quad n \geq 1, \quad (3)$$

where $X(0)$ denotes the initial system state.

Focusing on the infinite-horizon discounted cost criterion, the warehouse manager's problem is to choose a non-anticipating control (policy), denoted by $u = \{y(n), n \geq 1\}$, consisting of order vectors for each period. The associated expected total discounted cost can be written as follows:

$$J(x, u) = \mathbb{E}_x \left[\sum_{n=1}^{\infty} \gamma^{n-1} (f(X(n))) + c(y(n)) \right], \quad (4)$$

where $\gamma \in (0, 1)$ is the discount factor, and $\mathbb{E}_x[\cdot]$ denotes the expectation conditional on the initial state $X(0) = x$.

For every initial state x , we seek to find the optimal ordering policy that minimizes the total expected discounted cost (4). That is, we want to determine

$$J^*(x) := \inf_u J(x, u), \quad (5)$$

where the infimum is taken over the class of non-anticipating controls. As mentioned earlier, it is computationally prohibitive to solve (5) because the standard MDP-based techniques suffer from the curse of dimensionality. With this in mind, we next describe a continuous-time approximation of the foregoing problem.

Impulse Control Approximation. We now formally derive an impulse control approximation to the preceding inventory control problem. One can rewrite the stochastic dynamics of the inventory state process (3) as

$$X(N) = x + \sum_{n=1}^N y(n) - D(N), \quad N \geq 1. \quad (6)$$

The key simplification is to view the warehouse manager's problem in continuous time and allow him to place orders at any point in time. With slight abuse of notation, we define a new *continuous-time* process

$$X(t) = x + \sum_{\{j: \tau_j \leq t\}} y^{(j)} - D(t), \quad t \geq 0, \quad (7)$$

where the time t replaces N in Eq. (6) and $y^{(j)}$ represents the j th order placed at time τ_j . In addition, we approximate the cumulative demand process $D(\cdot)$ by a Gaussian process. To be specific, we assume

$$D(t) = \mu t + \sigma B(t), \quad t \geq 0, \quad (8)$$

where $B(\cdot)$ is a standard d -dimensional Brownian motion, $\mu \in \mathbb{R}^d$ is its drift vector, and $\sigma\sigma^\top$ is a positive-definite covariance matrix.

The warehouse manager's goal is to minimize the total expected discounted cost. More precisely, let $0 < \tau_1 < \tau_2 < \dots$ denote the sequence of strictly increasing, non-anticipating stopping times at which he places orders. Then, under the control policy $u = \{(y^{(j)}, \tau_j), j \geq 1\}$, the system state evolves according to the d -dimensional stochastic process

$$X^u(t) = x - \mu t - \sigma B(t) + \sum_{\{j: \tau_j \leq t\}} y^{(j)}, \quad t \geq 0. \quad (9)$$

Letting the annual interest rate be $r > 0$, the expected total discounted cost under policy u is given by

$$V(x, u) = \mathbb{E}_x \left[\int_0^\infty e^{-rt} f(X^u(t)) dt + \sum_j e^{-r\tau_j} c(y^{(j)}) \right]. \quad (10)$$

We then define the optimal value function as follows:

$$V(x) = \inf_{u \in \mathcal{U}} V(x, u) \text{ for each } x \in \mathbb{R}^d, \quad (11)$$

where the infimum is taken over the set \mathcal{U} of non-anticipating policies.

4. The HJB Equation and an Equivalent Stochastic Identity

In this section, we describe an identity, Eq. (15) below, that is similar in spirit to the results used by Han et al. (2018) to justify their deep BSDE method for solving semilinear PDEs. That earlier work provided the motivation for our approach, though the specifics of our approach to solving the impulse control problem differ significantly.

The value function V we seek in (11) can be characterized as the solution to a particular kind of highly nonlinear PDE, namely, the HJB equation associated with the impulse control problem. Using the infinitesimal dynamic programming principle, one can show formally that the value function V should satisfy the following HJB equation:

$$((\mathcal{L} + r) V - f)(x) \vee \left(V(x) - \inf_{y \in \mathbb{R}_+^d} (V(x + y) + c(y)) \right) = 0, \quad x \in \mathbb{R}^d, \quad (12)$$

where $\mathcal{L} := -\frac{1}{2} \cdot \text{Tr}(\sigma\sigma^\top \text{Hess}(V)) + \mu^\top \nabla V$ is the diffusion operator; ∇V and $\text{Hess}(V)$ denote the gradient and Hessian of V , respectively; and $a \vee b := \max\{a, b\}$ for scalars a and b . To elaborate, the first term on the left-hand side of Eq. (12), which we will refer to as the “no action” term, represents taking no action, which intuitively means that the warehouse manager opts to do nothing when the system state is x . The second term, which we will refer to as the “intervention” term, corresponds to placing an order when the system state is x , with the warehouse manager determining the order size vector y^* that minimizes future expected discounted costs.

The HJB equation (12) will not be used directly to learn the value function V in our approach. Instead, we rely on a related probabilistic characterization of V , to be described shortly in Eq. (15). To this end, we begin by specifying what we call a *reference policy* that is used to generate sample paths of the inventory process. That is, it facilitates our sampling of the paths living in the state space. We refer to the state process under the reference policy as the *reference process*, denoted by $\tilde{X}(\cdot)$. Roughly speaking, we choose a reference policy so that the reference process tends to occupy the parts of the state space that we expect the optimal policy to visit frequently.

As mentioned earlier, Johnson (1967) characterized the optimal policy for the SJRP as a (σ, S) policy. Also, for our approximating impulse control problem, a careful examination of the HJB equation (12) suggests that whenever an order is placed, the inventory vector is brought up to an order-up-to vector that is independent of the current inventory vector, provided the latter does not exceed the order-up-to vector (more will be said about this at the end of Section 5). Thus, we build on a (randomized) order-up-to policy for choosing a reference policy. Additionally, we set the order times under the reference policy as the event times of a Poisson process with rate λ . We let T_j denote the j th event time of the Poisson process for $j = 1, 2, \dots$. Given these event times, we let $Z_j \in \mathbb{R}^d$, for $j = 1, 2, \dots$, be random vectors drawn independently from a common distribution Φ . In particular, Z_j will serve as the (random) order-up-to vector for the j th order under the reference policy. That is, $(Z_j - \tilde{X}(T_j-))^+$ denotes the order quantity associated with the order-up-to vector Z_j ; here, $(x)^+$ denotes the componentwise positive parts of $x \in \mathbb{R}^d$, and $\tilde{X}(T_j-)$ denotes the inventory vector just before time T_j .

Randomizing the order-up-to vectors facilitates greater exploration of the state space and improves the training process. With this in mind, we let $(\zeta_j)_{j=1}^\infty$ denote a sequence of i.i.d random vectors in \mathbb{R}^d , whose components are independent exponential random variables with mean $\alpha_i = \alpha \mu_i / \lambda$

for $i = 1, \dots, d$. Then, we let

$$Y_j = \max \left\{ Z_j - \tilde{X}(T_j-), \zeta_j \right\},$$

denote the vector of order quantities of various items for the j th order, where the $\max\{\cdot, \cdot\}$ is applied componentwise. This adjustment guarantees positive order quantities even if $Z_j \not\geq \tilde{X}(T_j-)$, i.e., if Z_j does not dominate $\tilde{X}(T_j-)$ componentwise. In turn, that facilitates greater exploration of the state space. To ensure the stability of the reference process, we set $\lambda \mathbb{E}[\zeta_j] < \mu_i$ for $i = 1, \dots, d$, i.e., $\alpha < 1$. Further details of the reference process parameters will be described in Section 5. Given λ, Φ and α , we let

$$U(t; \alpha, \lambda, \Phi) = \sum_{j: T_j \leq t} Y_j, \quad t \geq 0, \quad (13)$$

and refer to the process $U(\cdot; \alpha, \lambda, \Phi)$ as the reference policy. When the context is clear, we suppress dependence on α , λ , and Φ , and simply write $U(\cdot)$. The corresponding reference process is given by

$$\tilde{X}(t) = x - \mu t - \sigma B(t) + U(t), \quad t \geq 0. \quad (14)$$

Stochastic identity. We now present the equivalent probabilistic representation of the value function V . Fix a reference policy $U(\cdot)$. Then, for any $T > 0$ and $\tilde{X}(0) = x \in \mathbb{R}^d$, $V(x)$ can be formally characterized as follows:

$$\begin{aligned} V(x) &= \sup \left\{ v \in \mathbb{R} : v - \int_0^T e^{-rt} \nabla V(\tilde{X}(t))^\top \sigma dB(t) \right. \\ &\leq e^{-rT} V(\tilde{X}(T)) + \int_0^T e^{-rt} f(\tilde{X}(t)) dt + \sum_{j: T_j \leq T} c(Y_j) e^{-rT_j}, \text{ a.s.} \left. \right\}. \end{aligned} \quad (15)$$

The right-hand side of Eq. (15) defines a stochastic target problem, which, roughly speaking, is a control problem that aims to steer the system state so as to hit a target set at the terminal time T . The connection between impulse control and stochastic target problems was first established in Bouchard (2009), for the case of discrete jump sizes. Kharroubi et al. (2010) later extended this connection for more general impulse control problems. We do not attempt a rigorous justification of the stochastic identity (15) in this paper; instead, we provide a formal derivation in Appendix A.

5. Computational Method

The identity (15) serves as the basis of our computational method. Seeking an approximate solution to it, we define the discretized loss function displayed in Eq. (17). Recall the reference process

defined in Eq. (14). As a preliminary to defining the loss function, we fix a partition $0 = t_0 < t_1 < \dots < t_N = T$ of the time horizon and simulate K discretized sample paths of the reference process at times t_0, t_1, \dots, t_N ; see Subroutine 1.

Reference policy. As reviewed in Section 2, decades of research activity has culminated in effective heuristic policies for the SJRP. These include the (R, S) , (Q, S) and can-order policies, which are described in Section 6 and Appendix C.2. We consider their performances as benchmarks for our proposed policy. Crucially, they each have an order-up-to vector S as a policy parameter. In what follows, we set

$$\mathbb{E}[Z_j] = S \quad \text{for } j \geq 1, \quad (16)$$

where S is derived for one of these three benchmark policies. More specifically, assuming the optimal order-up-to levels are positive,¹ we set Z_j to be a vector of lognormal random variables, where its i th component has mean S_i and variance $(\nu S_i)^2$. Here, $\nu > 0$ is a tuning parameter and is used to control the degree of exploration of the state space. Similarly, the parameter α that determines the means of the exponential random vectors ζ_j , for $j \geq 1$, is viewed as a tuning parameter.

Loss function. Our method, described in Algorithm 2, computes the loss function defined in Eq. (17) by summing over the sample paths of the reference process and over discrete time steps to approximate the various integrals over $[0, T]$ appearing in the identity (15). We approximate the value function $V(\cdot)$ and its gradient $\nabla V(\cdot)$ by deep neural networks, H_θ and G_ϑ , respectively, with associated parameter vectors θ and ϑ . Using the sample paths of the time-discretized reference process, the loss function L_β is defined as

$$\begin{aligned} L_\beta(\theta, \vartheta) := & \frac{1}{K} \sum_{k=1}^K \left[-H_\theta(x_0^{(k)}) + \beta \cdot l\left(H_\theta(x_0^{(k)}) - e^{-rT} H_\theta(\tilde{X}^{(k)}(T))\right) \right. \\ & \left. - \sum_{n=0}^{N-1} e^{-rt_n} G_\vartheta(\tilde{X}^{(k)}(t_n))^\top \sigma \Delta B^{(k)}(t_n) - \sum_{n=0}^{N-1} e^{-rt_n} f(\tilde{X}^{(k)}(t_n)) \Delta t_n - \sum_{n=0}^{N-1} e^{-rt_n} c(\Delta U^{(k)}(t_n)) \right], \end{aligned} \quad (17)$$

where the tuning parameter $\beta \gg 1$ can be viewed as a Lagrange multiplier. The penalty function $l(\cdot)$ is given by

$$l(x) = [(x)^+]^2. \quad (18)$$

¹This is a reasonable assumption for our test problems because the backlog costs are considerably larger than the holding cost.

Subroutine 1 Euler-Maruyama discretization scheme.

Input: A reference process $U(\cdot; \alpha, \lambda, \Phi)$, the drift vector μ , the covariance matrix $\sigma\sigma^\top$, the time horizon T , the number of intervals N , a discretization step size $\Delta t = T/N$, and an initial state x_0 .

Output: Discretized reference process $\tilde{X}(t_n)$ for $n = 1, \dots, N$, the Brownian increments $\Delta B(t_n)$ and compound Poisson increments $\Delta U(t_n)$ for $n = 0, \dots, N-1$.

```

1: function EULER-MARUYAMA( $T, \Delta t, x$ )
2:   Construct the partition  $0 = t_0 < \dots < t_N = T$ , where  $t_{n+1} = t_n + \Delta t$  for  $n = 0, \dots, N-1$ .
3:   Generate  $N$  i.i.d.  $d$ -dimensional Gaussian random vectors  $\Delta B(t_n)$  with mean vector zero
   and covariance matrix  $\Delta t I$  for  $n = 0, \dots, N-1$ .
4:   Generate  $N$  i.i.d.  $d$ -dimensional vectors  $Z_n$ , using  $\Phi$  whose components have independent
   lognormal distributions, for  $n = 0, \dots, N-1$ .
5:   Generate  $N$  i.i.d.  $d$ -dimensional vectors  $\zeta_n$  for  $n = 0, \dots, N-1$ , where each component is
   drawn independently from an exponential distribution with mean  $\alpha_i$ .
6:   for  $n = 0$  to  $N-1$  do
7:     Generate  $I_n \sim \text{Bernoulli}(\lambda \Delta t)$ 
8:      $\Delta U(t_n) \leftarrow I_n \cdot \max\{Z_n - \tilde{X}(t_n), \zeta_j\}$  (with  $\max\{\cdot, \cdot\}$  applied componentwise)
9:      $\tilde{X}(t_{n+1}) \leftarrow \tilde{X}(t_n) - \mu \Delta t - \sigma \Delta B(t_n) + \Delta U(t_n)$ 
10:   end for
11:   return  $\tilde{X}(t_n)$  for  $n = 0, \dots, N$ , and  $\Delta B(t_n)$  and  $\Delta U(t_n)$  for  $n = 0, \dots, N-1$ .
12: end function

```

The function L_β consists of (the negative of) the value function estimate, $-H_\theta(x_0^{(k)})$, and a penalty term, $\beta l(\cdot)$, averaged over K initial states $x_0^{(k)}$, $k = 1, \dots, K$. As mentioned in Step 6 of Algorithm 2, the process $\tilde{X}(\cdot)$ is simulated continuously, meaning that the terminal state of an iteration becomes the initial state of the next iteration. Loosely speaking, this approach can be seen as an attempt to capture the long-run behavior of the reference process. The penalty term penalizes violations of the almost sure inequality that appears in Eq. (15). The higher β is, the lower the violation probability is. Note from Eq. (15) that we seek to choose the largest value v while satisfying the inequality there almost surely. Thus, the loss function L_β is designed so that as we minimize it, we increase

the value function estimate H_θ , while simultaneously decreasing the violation probability. Also, we average over K initial states to avoid overfitting at any particular state. The tuning parameter β seeks to balance these two different objectives.

The penalty rate and learning rate schedules. Our computational method uses a stochastic gradient descent (SGD) type method to minimize the loss function. This involves choosing a learning rate schedule as done for deep learning algorithms. Additionally, we also need to choose the parameter β that is used to penalize the violations of the stochastic inequality on the right-hand side of Eq. (17). As one would expect, the higher the value of β , the lower the violation probability is. However, we observed empirically that the training is less stable with a higher value of β . To deal with this instability, we adopt the approach of gradually increasing the penalty parameter β during training, while decreasing the learning rate simultaneously. More specifically, we begin with a relatively low value of the penalty parameter β (and thus, we observe a significant violation of the stochastic inequality) while setting the learning rate parameter relatively large and iterate until the loss appears to converge. Then, we increase the penalty rate (e.g., by a factor of ten) and also decrease the learning rate parameter if needed, e.g., if we observe instability. Again, we iterate until the loss appears to converge. We keep increasing the penalty parameter in this manner until the violation probability is sufficiently low, e.g., less than 1%. For this final value of the penalty parameter, we choose a learning rate schedule manually by observing the evolution of the loss as we iterate, and lowering the learning rate as needed.

Using the approach thus described, and through extensive experimentation, we identified a set of *a priori* fixed penalty rate and learning rate schedules to be considered in our experiments, as reflected in Algorithm 2. In particular, for each run of the algorithm, the penalty rate schedule $\{\beta_1, \dots, \beta_M\}$ is fixed and regarded as part of the input to the algorithm. See Appendix B.2 for additional details on the specific penalty parameter and learning rate schedules used for our test problems. Further implementation details of our computational method are provided in Appendix B.

The proposed policy. After obtaining the neural network approximations H_θ and G_θ of the value function and its gradient, respectively, we propose a policy exploiting the structure of the HJB equation (12). To be specific, Eq. (12) implies that either the no action term is zero, i.e.,

$$\mathcal{L}V(x) + rV(x) - f(x) = 0, \quad (19)$$

Algorithm 2 Algorithm for approximating the value function of the impulse control problem.

Input: The number of iteration steps M , a batch size K , a time horizon T , the number of intervals N , a discretization step-size Δt , an initial state x_0 , a fixed reference policy $U(\cdot; \alpha, \lambda, \Phi)$, a penalty scheme $\{\beta_m\}$ and an optimization algorithm (e.g., SGD, ADAM, or RMSProp).

Output: The neural network approximation of the value function $V(\cdot)$, $H_\theta(\cdot)$, and of its gradient $\nabla V(\cdot)$, $G_\vartheta(\cdot)$.

- 1: Initialize the neural networks for $H_\theta(\cdot)$ and $G_\vartheta(\cdot)$. Set $x_0^{(k)} = x$ for all $k = 1, \dots, K$.
- 2: **for** $m \leftarrow 1$ to M **do**
- 3: For each sampled initial point $x_0^{(k)}$, simulate a discretized sample path of the inventory state process, Brownian motion increments, and increments of the compound Poisson process $\{\tilde{X}^{(k)}, \Delta B^{(k)}, \Delta U^{(k)}\}$ with a time horizon T and a step-size Δt , starting from $x_0^{(k)}$ by invoking EULER-MARUYAMA($T, \Delta t, x_0^{(k)}$) for $k = 1, \dots, K$.
- 4: Compute the Lagrangian function
$$L_{\beta_m}(\theta, \vartheta) = \frac{1}{K} \sum_{k=1}^K \left(-H_\theta(x_0^{(k)}) + \beta_m \left[\left(H_\theta(x_0^{(k)}) - e^{-rT} H_\theta(\tilde{X}^{(k)}(T)) \right. \right. \right. \\ \left. \left. \left. - \sum_{n=0}^{N-1} e^{-rt_n} G_\vartheta(\tilde{X}^{(k)}(t_n))^\top \sigma \Delta B^{(k)}(t_n) - \sum_{n=0}^{N-1} e^{-rt_n} f(\tilde{X}^{(k)}(t_n)) \Delta t - \sum_{n=0}^{N-1} e^{-rt_n} c(\Delta U^{(k)}(t_n)) \right] ^+ \right] ^2 \right)$$
- 5: Compute the gradient of the Lagrangian ∇L with respect to (θ, ϑ) and update using the chosen optimization algorithm.
- 6: Update the initial states by setting, for each $k = 1, \dots, K$, $x_0^{(k)} \leftarrow \tilde{X}^{(k)}(T)$.
- 7: **end for**
- 8: **return** Functions $H_\theta(\cdot)$ and $G_\vartheta(\cdot)$.

or the intervention term is zero, i.e.,

$$V(x) = \inf_{y \in \mathbb{R}_+^d} \{V(x + y) + c(y)\}. \quad (20)$$

In the former case, it is optimal to take no action. In the latter case, it is optimal to place an order, and the order vector is given by the minimizer of the right-hand side of Eq. (20).

One way to operationalize this is to check if condition (19) holds. If (19) holds for some state x , no action is required; otherwise, intervention through impulse control is warranted. That is, if for

our neural network estimates of V and ∇V , we have

$$\mathcal{L}V(x) + rV(x) - f(x) \leq -\epsilon < 0, \quad (21)$$

then we intervene through impulse control. Here ϵ is a suitably chosen numerical tolerance to account for optimization and sampling errors. To obtain an estimate of the value of $\mathcal{L}V$, note that estimates of the value function V and its gradient ∇V are already available from the deep neural network approximations, H_θ and G_ϑ , respectively. It then remains to estimate the Hessian of V through, for example, automatic differentiation of G_ϑ (Huré et al., 2020; Pham et al., 2021).

If one decides to intervene, the impulse control y^* is determined by selecting

$$y^* \in \operatorname{argmin}_{y \in \mathbb{R}_+^d} \{H_\theta(x + y) + c(y)\}. \quad (22)$$

To solve the minimization problem in (22), one can use a variety of numerical optimization techniques. Further details are provided in Appendix B.

We interpret this policy in the context of the original (discrete-time) formulation of the SJRP as follows: Given a system state x , the warehouse manager checks if an intervention is warranted. If so, he places an order, and his order vector is y^* given in Eq. (22).

Simulation and optimization. *A priori*, under the proposed policy, every time that the warehouse manager decides to place an order, he needs to solve the minimization problem in Eq. (22) to determine the order size vector y^* . This is computationally burdensome for performance simulations. However, the following observation allows us to compute a single order-up-to vector only once at the beginning of a simulation, resulting in a substantial speedup. Consider the minimization problem in Eq. (22). Because the inventory state x is not a decision variable, the problem is in fact equivalent to

$$\min_{y \in \mathbb{R}_+^d} \left\{ H_\theta(x + y) + c(y) + \sum_{i=1}^d c_i x_i \right\}, \quad (23)$$

which can be further simplified and bounded as follows:

$$\begin{aligned} \min_{y \in \mathbb{R}_+^d} \left\{ H_\theta(x + y) + c(y) + \sum_{i=1}^d c_i x_i \right\} &= \min_{y \in \mathbb{R}_+^d} \{H_\theta(x + y) + c(x + y)\} \\ &\geq \min_{z \in \mathbb{R}^d} \{H_\theta(z) + c(z)\}. \end{aligned} \quad (24)$$

Let z^* be the optimal solution to the minimization problem in Eq. (24). Then, as long as $x \leq z^*$ componentwise, the minimization problems in Eqs. (22) and (24) are equivalent. This in turn

implies that under our proposed policy, the order-up-to vector is simply z^* , irrespective of the initial state x_0 , as long as $x_0 \leq z^*$. Thus, if we assume that $z^* \geq 0$, which holds in all our test problems, then, since we start our simulations from the initial state $x_0 = 0$, the order-up-to vector z^* does not need to be recomputed at every ordering decision.

An alternative approach for deriving the optimal order quantity. One can alternatively use the neural network approximation of the gradient, G_ϑ , for solving (22). In particular, the first-order optimality condition yields $\nabla_z V(z) = -c$, where c is the vector of variable ordering costs. Thus, substituting G_ϑ for ∇V then yields

$$G_\vartheta(z^*) = -c. \quad (25)$$

Solving this system gives the optimal order-up-to vector. This alternative procedure sometimes resulted in better-performing policies in our experiments.

6. Test Problems and Benchmark Policies

We begin by describing the test problems. We consider a total of 43 test problems² that can be divided into three groups. First, we consider 27 twelve-dimensional problems based on an example studied in Atkins and Iyogun (1988). These problems vary across three attributes: demand variability, fixed ordering cost, and backlog penalty costs. For each attribute, we consider low, medium, and high values, yielding 27 test problems.

Computing the optimal policy for these problems is intractable due to the curse of dimensionality. Thus, to assess the performance of our proposed policy, we use the state-of-the-art heuristic policies drawn from the literature as benchmarks; see below for more on those benchmark policies. However, when the number of items is small, e.g., $d = 2$, one can compute the optimal policy using standard dynamic programming methods. This, of course, helps assess how close our proposed policy is to the optimal one for low-dimensional problems. Therefore, we next consider 7 test problems of dimension two. To do so, we consider only two products of the 12-dimensional problem. For our base case of the two-dimensional test problems, we choose the medium values of demand variability, ordering cost, and backlog penalty costs. Additionally, while fixing all else we consider setting each

²Additionally, Appendix D considers a one-dimensional impulse control problem studied in Sulem (1986) and verifies the validity of our solution method by comparing it to the one derived in Sulem (1986); see Figure 3 in Appendix D.

of the three attributes, one at a time, to low and high values, resulting in a total of seven test problems of dimension two. Lastly, to assess the scalability of our method, we consider nine test problems of dimension 50 that are designed by building on the earlier test problems. More will be said about them below.

For all test problems, we set the time unit as a year, the initial inventory to zero, and the annual interest rate to $r = 5\%$, and allow the warehouse manager to make ordering decisions weekly.

12-dimensional test problems. We build on the 12-item problem studied in Atkins and Iyogun (1988). We set the holding cost parameters $h_i = 2$ for all items ($i = 1, \dots, 12$). To capture the three levels of demand variability, we proceed as follows: For low variability, we model the item-level demand as independent Poisson processes. In this case, the coefficient of variation (CV) of item-level annual demand ranges from 0.158 (for items with annual demand rate 40) to 0.224 (for items with annual demand rate 20); cf. Table 1. For medium and high variability cases, we model each item-level annual demand as an independent negative binomial random variable, and set their parameters so that the CV of the annual demand is 0.5 per item for the medium variability case, and it is 1 per item for the high-variability case. We choose the negative binomial distribution because it can effectively model both high and low demand rates, and its dispersion parameter can be used to fit a wide range of empirical retail demand distributions (Nahmias and Smith, 1994; Ehrhardt, 1979). Table 1 shows the annual demand rates and variable costs for each item. As mentioned earlier, we consider three possible values for the fixed cost of ordering and the backlog penalty costs. More specifically, we set $p_i = p$ for all i and let $p \in \{10, 50, 100\}$ and $c_0 \in \{20, 100, 200\}$.

Table 1: Demand rates and variable costs for the 12-item problem

Item	1	2	3	4	5	6	7	8	9	10	11	12
Demand rate	40	35	40	40	40	20	20	20	28	20	20	20
c_i	0.1	0.1	0.2	0.2	0.4	0.2	0.4	0.4	0.6	0.6	0.8	0.8

Low-dimensional test problems. Letting $d = 2$, the parameters of our test problem are taken from the preceding one. Namely, we focus on items 1 and 7 there. For the base case, we set $c_0 = 50$ and $p = 50$, and model item-level annual demand as a negative binomial random variable with annual CV = 0.5, i.e., the medium variability case. The other six 2-dimensional test problems follow from varying one of the following at a time: the demand variability, the fixed cost of ordering, and the backlog penalty parameter. More specifically, these alternative parameters correspond to demand variability $\in \{\text{low, high}\}$, $c_0 \in \{20, 100\}$, and $p \in \{10, 100\}$. For the low variability case, we model the item-level demands as independent Poisson processes as done earlier.

High-dimensional test problems. As mentioned earlier, we also consider nine 50-dimensional test problems. To set the problem parameters, we partition the items into three groups. To be specific, items 1-15 form the first group, items 16-30 form the second group, and items 31-50 form the third group. Within each group, items share the same annual demand rate, per-unit holding cost, backlog penalty, and variable cost; these parameters differ across groups. We vary the fixed cost $c_0 \in \{50, 150, 250\}$, and again model demand as Poisson (low variability) or negative binomial with an item-level CV of 0.5 or 1.0 (for moderate and high variability). These lead to nine additional test problems. Table 2 summarizes the key parameters for each group.

Table 2: Problem parameters for the 50-item test case (annual demand rates and holding and backlog costs).

Items	1–15	16–30	31–50
Demand rate	50.0	25.0	12.5
h_i	1.0	2.0	4.0
p_i	25.0	50.0	100.0
c_i	0.1	0.2	0.4

Next, we describe the benchmark policies we use to assess the performance of our proposed policy. Crucially, we make all performance comparisons in the context of the original discrete-time formulation, cf. Eqs. (1)–(5), as opposed to the impulse control approximation (7)–(11), even

though our proposed policy is derived using the latter.

Benchmark policies. As mentioned earlier, it is computationally feasible to solve the low-dimensional test problems. Thus, we compute the optimal policy using policy iteration and use it as the benchmark for those cases. For the other test problems, we rely on effective heuristic policies drawn from the extensive literature on the SJRP. More specifically, we consider the following benchmark policies:

- (i) the periodic review (R, S) policy proposed by Atkins and Iyogun (1988);
- (ii) the (Q, S) policy described in Pantumsinchai (1992);
- (iii) the can-order policy described in Federgruen et al. (1984);
- (iv) the independent (s, S) control policy (Sulem, 1986; Zheng and Federgruen, 1991);

Under the (R, S) policy, the inventory levels of all items are replenished every R time periods, with each item $i = 1, \dots, d$ having its inventory level brought back to its target S_i . The (Q, S) policy, studied in Pantumsinchai (1992), places an order whenever the total aggregate demand since the previous replenishment exceeds a specified value Q , raising the inventory, for each item $i = 1, \dots, d$, back to its order-up-to level S_i . In the can-order policy, each item i is managed with three control parameters: a reorder point s_i , a can-order level c_i , and an order-up-to level S_i . For each item $i = 1, \dots, d$, a replenishment is triggered when its inventory level drops to or below s_i , bringing it back up to S_i . If at this point the inventory level of any other item $j \neq i$ is at or below its can-order level c_j , this item j is also included in the replenishment, and its inventory is raised to S_j . The independent (s, S) policy assumes the setting without any benefits from joint ordering and calculates the individual optimal (s, S) levels as if there were no opportunity for group savings on the fixed cost. Further implementation details of these benchmark policies are provided in Appendix C.2.

7. Computational Results

For the test problems introduced in Section 6, we now compare the performance of our proposed policy, henceforth referred to as the neural network (NN) policy, to the benchmarks. For the benchmark policies, i.e., (R, S) , (Q, S) , can-order, and independent (s, S) , we compute their performance estimates by averaging over 10,000 sample paths of length 10,000 time periods each. The resulting

standard errors are negligible ($\leq 0.01\%$ of the respective estimated performance), so we do not report them. For the NN policy, depending on the problem dimension and demand variability, we estimate its performance by averaging over 10, 100, or 10,000 sample paths of length 10,000 periods each; more details are provided in the sequel. The numbers of simulated sample paths under the NN policy are chosen to strike a balance between computational tractability and statistical accuracy: On the one hand, checking the no-action condition Ineq. (21) is computationally intensive, as it involves evaluating the approximate Hessian of the value function through automatic differentiation; on the other hand, we simulate enough paths to obtain standard errors that are less than 1% of the respective estimated performance. For a test problem, we say that the NN policy *matches* a benchmark if the estimated benchmark cost is within 1% of the estimated cost under the NN policy, i.e.,

$$\frac{|\text{Estimated benchmark cost} - \text{Estimated NN cost}|}{\text{Estimated NN cost}} \leq 1\%,$$

and that the NN policy *beats* a benchmark if the estimated benchmark cost is at least 1% more than the estimated NN cost, i.e.,

$$\frac{\text{Estimated benchmark cost} - \text{Estimated NN cost}}{\text{Estimated NN cost}} > 1\%.$$

On the current hardware configuration, it takes approximately one to two hours to simulate a single trace in 12 dimensions, and roughly three to four hours in 50 dimensions. In 12 dimensions, neural network training completes in under two hours, whereas in 50 dimensions, it takes about five hours. Further implementation details, such as machine configurations, programming language, and software packages, are described in Appendix B.1. Our code is available at <https://github.com/wvaneeke/StochasticJRP>.

Before presenting the computational results in detail, we first summarize the main findings. Overall, the NN policy performs strongly and often surpasses the benchmarks by a significant margin. Across the 36 high-dimensional test problems (27 in dimension twelve and 9 in dimension fifty), it matches or beats the best benchmark, and does so by a clear margin in most medium- to high-variability cases. In all seven two-dimensional test problems, the performance gap between the NN policy and the MDP solution is within 1%, and the NN policy structure closely aligns with that of the MDP, suggesting that the NN policy learns the optimal policy in low dimensions. We now proceed to the detailed results.

Results in dimension 12. Tables 3, 4, and 5 report computational results in the low, medium, and high variability settings, respectively, for the main 12-dimensional test problems. Each table reports the simulated performances of our NN policy, together with relative gaps between the various benchmark policies and our policy. The performance of the NN policy is estimated by averaging over 10 sample paths in the low- and medium-variability cases, and over 100 sample paths in the high-variability cases. The standard errors are shown as percentages of the estimated averages. Reported standard errors are small ($< 1\%$), indicating statistically reliable estimates.

For the nine test problems with low variability in Table 3, our NN policy performs on par with the best benchmark policy, which turns out to be the (Q, S) policy in all cases. The NN policy outperforms the can-order policy by a significant margin in most cases, but the performance gap shrinks as the backlog penalty increases. Intuitively, the shrinking performance gaps can be explained by the can-order policy’s tendency to order more proactively than other benchmark policies, suggesting that it is better at avoiding states with large backlogs and performs better as the backlog penalty increases. The NN policy also significantly outperforms the independent (s, S) policy. This is expected, as the independent (s, S) policy does not exploit cost-saving opportunities of joint replenishment and instead triggers an order each time an item reaches its reorder point individually.

We now focus on the performance comparisons among NN, (R, S) , and (Q, S) in Table 3. For all values of the fixed cost, the NN policy tends to perform better when compared to (R, S) and (Q, S) , as the backlog penalty increases. A possible explanation is that the neural networks are flexible enough to learn the shape of the ordering boundary well, so under high backlog penalties, the NN policy can better avoid costly states with large backlogs. When the fixed cost is high, it is optimal to place orders less frequently, allowing demand to pool between replenishments and thereby reducing effective variability. In this regime, the system behaves nearly deterministically, and we expect (Q, S) and (R, S) to be close to optimal. The intuition that (R, S) is near-optimal is threefold: (i) infrequent orders imply that aggregate inter-order demand is less variable, bringing the system closer to being deterministic; (ii) in a deterministic setting, it is optimal to place orders at regularly spaced times; and (iii) if optimal order times are approximately regular, a policy that optimizes order-up-to levels and (deterministic) review times, namely (R, S) , is near-optimal. The slight advantage of (Q, S) over (R, S) likely stems from its additional adaptivity in timing orders.

Consequently, in a system with low effective variability (low demand variability and large fixed cost), there is little headroom for the NN policy to improve upon these benchmarks.

In the medium-variability setting (Table 4), the NN policy often delivers sizable gains over (Q, S) and (R, S) , with the advantage growing as the backlog penalty increases. This aligns with the intuitive explanation discussed in the low-variability setting: the NN policy appears to learn the ordering boundary more accurately. The NN policy also dominates can-order in all cases, though the performance gap narrows as backlog penalties rise; again this observation is consistent with our earlier explanation on can-order’s proactive replenishment. Finally, as expected, the NN policy substantially outperforms the independent (s, S) policy. In the high-variability setting (Table 5), the qualitative pattern is similar to the medium-variability cases, with the NN policy matching or beating the best benchmark in all cases, and often with high margins.

Table 3: Computational results for $d = 12$ with Poisson demand and $h = 2.0$ (standard errors shown as percentage of simulation average; other entries are percentage gaps vs. NN policy, with standard errors in percentage points).

c_0	p	Cost of NN Policy	Cost of Other Policies (Relative to NN Policy)			
			(R, S)	(Q, S)	Can-Order	Ind. (s, S)
20	10	$6285.08 \pm 0.28\%$	$0.02\% \pm 0.28\%$	$-0.87\% \pm 0.28\%$	$20.14\% \pm 0.34\%$	$155.21\% \pm 0.71\%$
	50	$7307.79 \pm 0.23\%$	$1.20\% \pm 0.23\%$	$-0.26\% \pm 0.23\%$	$10.12\% \pm 0.25\%$	$148.22\% \pm 0.57\%$
	100	$7552.95 \pm 0.26\%$	$3.44\% \pm 0.27\%$	$1.76\% \pm 0.26\%$	$8.36\% \pm 0.28\%$	$147.12\% \pm 0.64\%$
100	10	$10243.10 \pm 0.26\%$	$-0.17\% \pm 0.26\%$	$-0.85\% \pm 0.26\%$	$8.31\% \pm 0.28\%$	$176.80\% \pm 0.72\%$
	50	$11852.35 \pm 0.39\%$	$1.26\% \pm 0.39\%$	$0.08\% \pm 0.39\%$	$6.89\% \pm 0.42\%$	$168.21\% \pm 1.05\%$
	100	$12332.85 \pm 0.30\%$	$2.49\% \pm 0.31\%$	$1.24\% \pm 0.30\%$	$5.85\% \pm 0.32\%$	$163.24\% \pm 0.79\%$
200	10	$13148.02 \pm 0.20\%$	$0.02\% \pm 0.20\%$	$-0.55\% \pm 0.20\%$	$6.77\% \pm 0.21\%$	$188.17\% \pm 0.58\%$
	50	$15089.08 \pm 0.28\%$	$1.69\% \pm 0.29\%$	$0.68\% \pm 0.28\%$	$5.54\% \pm 0.30\%$	$181.57\% \pm 0.79\%$
	100	$15808.96 \pm 0.41\%$	$1.99\% \pm 0.42\%$	$0.85\% \pm 0.41\%$	$5.19\% \pm 0.43\%$	$175.64\% \pm 1.12\%$

Table 4: Computational results for $d = 12$ with negative binomial demand (CV = 0.5) and $h = 2.0$ (standard errors shown as percentage of simulation average; other entries are percentage gaps vs. NN policy, with standard errors in percentage points).

c_0	p	Cost of NN Policy	Cost of Other Policies (Relative to NN Policy)			
			(R, S)	(Q, S)	Can-Order	Ind. (s, S)
20	10	$8217.34 \pm 0.67\%$	$6.64\% \pm 0.71\%$	$0.15\% \pm 0.67\%$	$14.64\% \pm 0.77\%$	$49.07\% \pm 1.00\%$
	50	$10585.13 \pm 0.78\%$	$20.84\% \pm 0.94\%$	$10.95\% \pm 0.87\%$	$1.26\% \pm 0.79\%$	$30.05\% \pm 1.01\%$
	100	$11409.81 \pm 0.74\%$	$28.58\% \pm 0.95\%$	$17.99\% \pm 0.87\%$	$4.00\% \pm 0.77\%$	$29.80\% \pm 0.96\%$
100	10	$12933.56 \pm 0.53\%$	$6.03\% \pm 0.56\%$	$2.08\% \pm 0.54\%$	$21.08\% \pm 0.64\%$	$96.45\% \pm 1.03\%$
	50	$16623.94 \pm 0.91\%$	$14.55\% \pm 1.04\%$	$8.46\% \pm 0.99\%$	$5.34\% \pm 0.96\%$	$65.26\% \pm 1.50\%$
	100	$17574.15 \pm 0.60\%$	$21.50\% \pm 0.73\%$	$14.61\% \pm 0.69\%$	$2.66\% \pm 0.62\%$	$59.82\% \pm 0.96\%$
200	10	$16586.35 \pm 0.81\%$	$2.90\% \pm 0.83\%$	$-0.14\% \pm 0.81\%$	$20.28\% \pm 0.97\%$	$113.84\% \pm 1.73\%$
	50	$20957.45 \pm 0.47\%$	$10.62\% \pm 0.52\%$	$5.93\% \pm 0.50\%$	$5.94\% \pm 0.50\%$	$82.37\% \pm 0.86\%$
	100	$21936.83 \pm 0.34\%$	$17.47\% \pm 0.40\%$	$12.01\% \pm 0.38\%$	$2.56\% \pm 0.35\%$	$76.44\% \pm 0.60\%$

Table 5: Computational results for $d = 12$ with negative binomial demand (CV = 1.0) and $h = 2.0$ (standard errors shown as percentage of simulation average; other entries are percentage gaps vs. NN policy, with standard errors in percentage points).

c_0	p	Cost of NN Policy	Cost of Other Policies (Relative to NN Policy)			
			(R, S)	(Q, S)	Can-Order	Ind. (s, S)
20	10	$8436.41 \pm 0.31\%$	$22.87\% \pm 0.38\%$	$1.23\% \pm 0.31\%$	$19.46\% \pm 0.37\%$	$31.66\% \pm 0.41\%$
	50	$13484.69 \pm 0.32\%$	$41.19\% \pm 0.45\%$	$21.31\% \pm 0.39\%$	$0.45\% \pm 0.32\%$	$7.58\% \pm 0.34\%$
	100	$16383.59 \pm 0.35\%$	$46.19\% \pm 0.51\%$	$33.25\% \pm 0.47\%$	$0.01\% \pm 0.35\%$	$8.07\% \pm 0.38\%$
100	10	$15481.77 \pm 0.32\%$	$17.50\% \pm 0.38\%$	$2.41\% \pm 0.33\%$	$24.70\% \pm 0.40\%$	$57.61\% \pm 0.50\%$
	50	$22399.89 \pm 0.31\%$	$39.22\% \pm 0.43\%$	$17.72\% \pm 0.36\%$	$1.48\% \pm 0.31\%$	$23.49\% \pm 0.38\%$
	100	$23969.84 \pm 0.32\%$	$57.83\% \pm 0.50\%$	$35.57\% \pm 0.43\%$	$1.62\% \pm 0.32\%$	$23.67\% \pm 0.39\%$
200	10	$20244.86 \pm 0.31\%$	$14.47\% \pm 0.35\%$	$2.64\% \pm 0.32\%$	$25.20\% \pm 0.39\%$	$70.88\% \pm 0.53\%$
	50	$28482.72 \pm 0.31\%$	$33.24\% \pm 0.41\%$	$15.42\% \pm 0.36\%$	$2.12\% \pm 0.32\%$	$34.73\% \pm 0.42\%$
	100	$30152.86 \pm 0.33\%$	$49.90\% \pm 0.49\%$	$30.75\% \pm 0.43\%$	$1.13\% \pm 0.33\%$	$32.83\% \pm 0.44\%$

Low-dimensional results. Table 6 and Figures 1 and 2 summarize our computational results in the two-dimensional test problems. To estimate performance of the NN policy, we average over 10,000 sample paths, each of length 10,000 periods, similar to what we do for the other benchmark policies. As mentioned earlier, the NN performance estimates are within 1% of the MDP solutions. Across the base case (Figure 1) and the six variants (Figure 2), the NN policy closely tracks the MDP solution: the decision boundaries largely overlap (dense purple regions), with minor local deviations near extremely-valued states. These visual observations are consistent with the small optimality gaps in Table 6 ($\approx 0.69\% - 1.02\%$ across cases), indicating that not only does the NN policy perform near-optimally when starting from the zero inventory state, but it also captures the geometry of the optimal policy. Among the benchmark policies, the can-order policy performs the best and closely matches the MDP solution in all seven test problems. It performs slightly better than the NN policy in the low fixed cost case ($c_0 = 20$) and the high backlog penalty case ($p = 100$). As explained earlier, intuitively, the can-order policy’s proactive replenishment is effective in cases involving high backlog penalties. Similarly, in the case of low fixed cost, a proactive replenishment policy, such as can-order, can be also expected to perform well.

Table 6: Computational results for the 2-dimensional test problems (simulation results are based on 10,000 sample paths, each consisting of 10,000 periods)

Test Instance	Cost of MDP Policy	Cost of NN Policy	Optimality Gap	(R, S)	(Q, S)	Can-Order	Ind. (s, S)
Base Case	2936.24 ± 1.14	2960.75 ± 1.12	$0.83\% \pm 0.02\%$	4337.42 ± 3.05	4356.86 ± 0.91	2965.83 ± 1.16	3380.97 ± 1.16
Low CV	2606.71 ± 0.39	2627.84 ± 0.41	$0.81\% \pm 0.01\%$	2869.85 ± 0.58	2778.16 ± 0.37	2705.03 ± 0.39	3295.64 ± 0.49
High CV	3120.60 ± 2.07	3152.36 ± 2.00	$1.02\% \pm 0.09\%$	7052.55 ± 7.77	6993.23 ± 1.90	3233.83 ± 2.32	3425.45 ± 2.37
$c_0 = 20$	2066.62 ± 0.82	2084.90 ± 0.81	$0.88\% \pm 0.01\%$	3271.59 ± 2.33	3298.85 ± 0.67	2069.63 ± 0.82	2287.05 ± 0.84
$c_0 = 100$	3931.67 ± 1.53	3958.84 ± 1.50	$0.69\% \pm 0.02\%$	5471.95 ± 4.14	5445.30 ± 1.28	3976.59 ± 1.54	4654.87 ± 1.58
$p = 10$	2572.19 ± 0.98	2595.98 ± 0.96	$0.93\% \pm 0.02\%$	3184.27 ± 1.63	2926.27 ± 0.93	2638.80 ± 1.02	3064.60 ± 1.04
$p = 100$	3071.69 ± 1.25	3099.26 ± 1.26	$0.90\% \pm 0.01\%$	4814.61 ± 4.27	4959.34 ± 0.96	3079.92 ± 1.25	3518.90 ± 1.27

Results in dimension 50. Finally, we turn to the 50-dimensional test problems. We estimate NN performance by averaging over 10 sample paths per test problem. Standard errors are small ($\approx 0.12\% - 0.66\%$), indicating reliable estimates. The NN policy beats the best benchmark in all cases, with performance gaps up to 6.79%. Under low variability, NN performs comparably

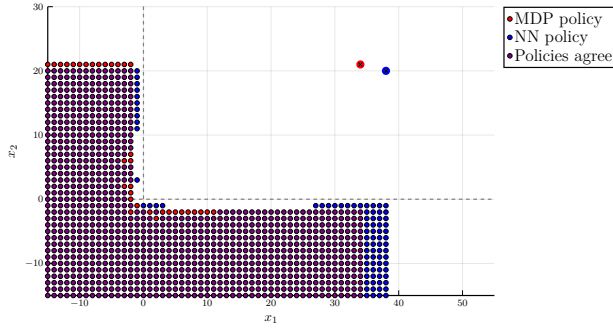


Figure 1: MDP and neural network policies (base case $d = 2$).

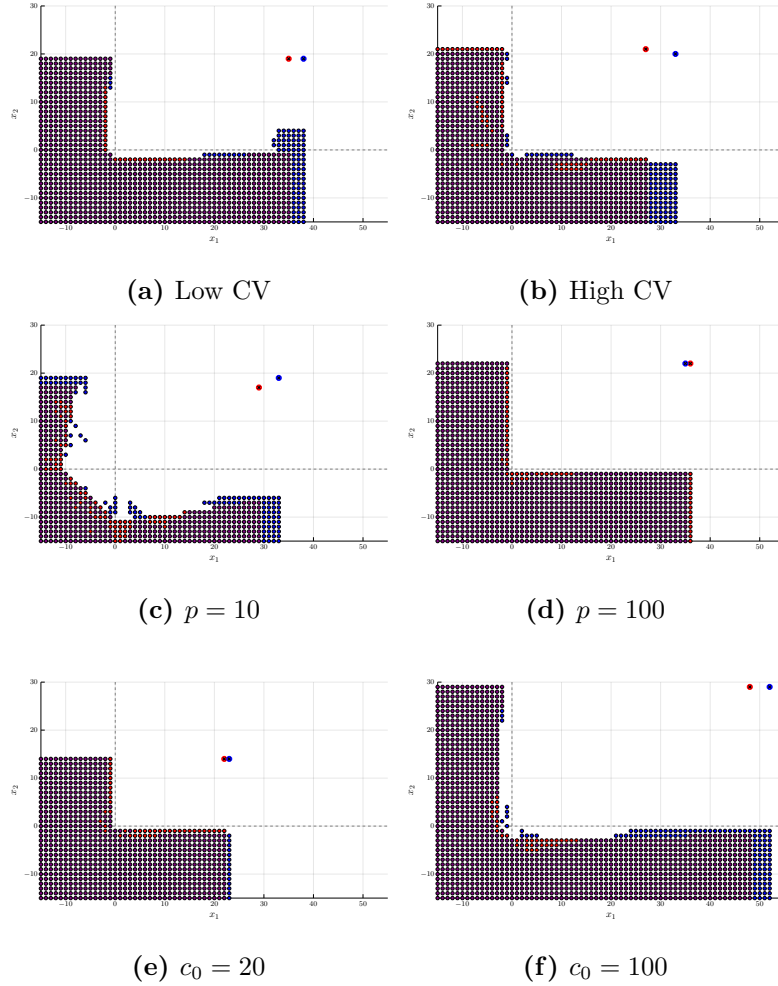


Figure 2: Comparison of MDP and neural network policies across the remaining six two-dimensional test problems.

to (R, S) and (Q, S) , while clearly outperforming can-order and independent (s, S) policies. As variability increases, NN's advantage over (R, S) and (Q, S) generally widens, whereas gaps versus can-order and independent (s, S) remain relatively stable.

Table 7: Computational results for $d = 50$ with $h = 2.0$ (standard errors shown as percentage of simulation average; other entries are percentage gaps vs. NN policy, with standard errors in percentage points).

CV	c_0	Cost of NN Policy	Cost of Other Policies (Relative to NN Policy)			
			(R, S)	(Q, S)	Can-Order	Ind. (s, S)
Poisson	50	$21834.88 \pm 0.12\%$	$1.06\% \pm 0.12\%$	$0.64\% \pm 0.12\%$	$25.27\% \pm 0.15\%$	$179.21\% \pm 0.34\%$
	150	$30507.63 \pm 0.12\%$	$0.87\% \pm 0.12\%$	$0.58\% \pm 0.12\%$	$16.20\% \pm 0.14\%$	$263.92\% \pm 0.44\%$
	250	$36237.30 \pm 0.13\%$	$0.91\% \pm 0.13\%$	$0.59\% \pm 0.13\%$	$20.56\% \pm 0.16\%$	$299.78\% \pm 0.52\%$
0.5	50	$36193.02 \pm 0.22\%$	$7.48\% \pm 0.24\%$	$4.45\% \pm 0.23\%$	$15.01\% \pm 0.25\%$	$75.78\% \pm 0.39\%$
	150	$48476.54 \pm 0.31\%$	$5.35\% \pm 0.33\%$	$3.32\% \pm 0.32\%$	$20.30\% \pm 0.37\%$	$136.25\% \pm 0.73\%$
	250	$56282.63 \pm 0.39\%$	$4.21\% \pm 0.41\%$	$2.60\% \pm 0.40\%$	$20.52\% \pm 0.47\%$	$166.85\% \pm 1.04\%$
1.0	50	$51855.77 \pm 0.60\%$	$15.83\% \pm 0.69\%$	$4.14\% \pm 0.62\%$	$14.29\% \pm 0.69\%$	$27.00\% \pm 0.76\%$
	150	$72289.70 \pm 0.66\%$	$16.22\% \pm 0.77\%$	$6.79\% \pm 0.70\%$	$23.15\% \pm 0.81\%$	$60.34\% \pm 1.06\%$
	250	$86029.32 \pm 0.51\%$	$13.92\% \pm 0.58\%$	$6.21\% \pm 0.54\%$	$23.89\% \pm 0.63\%$	$77.26\% \pm 0.90\%$

8. Concluding Remarks

In this paper, we tackle a classical inventory control problem in high dimensions by formulating it as an impulse control problem and approximating its solution via deep-learning techniques. Through extensive hyperparameter tuning, a tailored training algorithm, and careful engineering of policy extraction, we were able to match or beat the best available benchmarks. Our approach not only provides effective solutions to the SJRP, but also opens up avenues for applying these numerical methods to broader classes of impulse control problems. In particular, the techniques developed here may be used to tackle impulse control problems in other fields, most promisingly in financial engineering—for example, cash flow management and investment decisions (Altarovici et al., 2017; Liu, 2004). Looking further ahead, it seems natural to extend our methodology to more complex supply-chain models, such as those with demand spillovers between facilities. We

leave these explorations for future work.

References

Adelman, D. and Klabjan, D. (2005). Duality and existence of optimal policies in generalized joint replenishment. *Mathematics of Operations Research*, 30(1):28–50.

Adelman, D. and Klabjan, D. (2012). Computing near-optimal policies in generalized joint replenishment. *INFORMS Journal on Computing*, 24(1):148–164.

Aksoy, Y. and Erenguc, S. (1988). Multi-item inventory models with co-ordinated replenishments: A survey. *International Journal of Operations & Production Management*, 8(1):63–73.

Altarovici, A., Reppen, M., and Soner, H. M. (2017). Optimal consumption and investment with fixed and proportional transaction costs. *SIAM Journal on Control and Optimization*, 55(3):1673–1710.

Applebaum, D. (2009). *Lévy Processes and Stochastic Calculus*. Cambridge University Press.

Ata, B., Harrison, J. M., and Si, N. (2024a). Drift control of high-dimensional reflected Brownian motion: A computational method based on neural networks. *Stochastic Systems*.

Ata, B., Harrison, J. M., and Si, N. (2024b). Singular control of (reflected) Brownian motion: A computational method suitable for queueing applications. *Queueing Systems*, pages 1–37.

Ata, B. and Kasikaralar, E. (2023). Dynamic scheduling of a multiclass queue in the Halfin-Whitt regime: A computational approach for high-dimensional problems. *Available at SSRN 4649551*.

Ata, B., Li, C., and Si, N. (2024c). Dynamic control of a make-to-order manufacturing system under throughput time constraints: An effective computational method in the high-dimensional case. Working paper.

Ata, B. and Xu, Y. (2025). Dynamic control of stochastic matching systems in heavy-traffic: An effective computational method for high-dimensional problems. Working paper.

Ata, B. and Zhou, Y. (2024). Analysis and improvement of eviction enforcement. Working paper.

Atkins, D. R. and Iyogun, P. O. (1988). Periodic versus “can-order” policies for coordinated multi-item inventory systems. *Management Science*, 34(6):791–796.

Azimzadeh, P., Bayraktar, E., and Labahn, G. (2018). Convergence of implicit schemes for Hamilton–Jacobi–Bellman quasi-variational inequalities. *SIAM Journal on Control and Optimization*, 56(6):3994–4016.

Azimzadeh, P. and Forsyth, P. A. (2016). Weakly chained matrices, policy iteration, and impulse control. *SIAM Journal on Numerical Analysis*, 54(3):1341–1364.

Balintfy, J. L. (1964). On a basic class of multi-item inventory problems. *Management Science*, 10(2):287–297.

Bayraktar, E., Cohen, A., and Nellis, A. (2023). A neural network approach to high-dimensional optimal switching problems with jumps in energy markets. *SIAM Journal on Financial Mathematics*, 14(4):1028–1061.

Beck, C., Hutzenthaler, M., Jentzen, A., and Kuckuck, B. (2022). An overview on deep learning-based approximation methods for partial differential equations. *arXiv preprint arXiv:2012.12348*.

Beckmann, M. (1961). An inventory model for arbitrary interval and quantity distributions of demand. *Management Science*, 8(1):35–57.

Bensoussan, A. and Lions, J. L. (1984). *Impulse Control and Quasi-Variational Inequalities*.

Bensoussan, A., Liu, R., and Sethi, S. P. (2005). Optimality of an (s, S) policy with compound Poisson and diffusion demands: A quasi-variational inequalities approach. *SIAM Journal on Control and Optimization*, 44(5):1650–1676.

Bertsekas, D. P. (2012). *Dynamic Programming and Optimal Control*, volume II. Athena Scientific, 4th edition.

Bezanson, J., Edelman, A., Karpinski, S., and Shah, V. B. (2017). Julia: A fresh approach to numerical computing. *SIAM Review*, 59(1):65–98.

Biagini, F., Gonon, L., and Reitsam, T. (2023). Neural network approximation for superhedging prices. *Mathematical Finance*, 33(1):146–184.

Bouchard, B. (2009). A stochastic target formulation for optimal switching problems in finite horizon. *Stochastics: An International Journal of Probability and Stochastics Processes*, 81(2):171–197.

Buehler, H., Gonon, L., Teichmann, J., and Wood, B. (2019). Deep hedging. *Quantitative Finance*, 19(8):1271–1291.

Chessari, J., Kawai, R., Shinozaki, Y., and Yamada, T. (2023). Numerical methods for backward stochastic differential equations: A survey. *Probability Surveys*, 20:486–567.

Constantinides, G. M. (1976). Stochastic cash management with fixed and proportional transaction costs. *Management Science*, 22(12):1320–1331.

Creemers, S. and Boute, R. (2022). The joint replenishment problem: Optimal policy and exact evaluation method. *European Journal of Operational Research*, 302(3):1175–1188.

Dixit, V. K. and Rackauckas, C. (2023). Optimization.jl: A unified optimization package.

E, W., Han, J., and Jentzen, A. (2017). Deep learning-based numerical methods for high-dimensional parabolic partial differential equations and backward stochastic differential equations. *Communications in Mathematics and Statistics*, 5(4):349–380.

E, W., Han, J., and Jentzen, A. (2021). Algorithms for solving high dimensional PDEs: From nonlinear Monte Carlo to machine learning. *Nonlinearity*, 35(1):278.

Ehrhardt, R. (1979). The power approximation for computing (s, S) inventory policies. *Management Science*, 25(8):777–786.

Federgruen, A., Groenevelt, H., and Tijms, H. C. (1984). Coordinated replenishments in a multi-item inventory system with compound Poisson demands. *Management Science*, 30(3):344–357.

Federgruen, A. and Zheng, Y.-S. (1992). The joint replenishment problem with general joint cost structures. *Operations Research*, 40(2):384–403.

Gallego, G. and Sethi, S. (2005). K-convexity in \mathbb{R}^n . *Journal of Optimization Theory and Applications*, 127(1).

Goyal, S. and Belton, A. (1979). Note on “A simple method of determining order quantities in joint replenishments under deterministic demand”. *Management Science*, 25(6):604.

Goyal, S. K. and Satir, A. T. (1989). Joint replenishment inventory control: Deterministic and stochastic models. *European Journal of Operational Research*, 38(1):2–13.

Han, J., Jentzen, A., and E, W. (2018). Solving high-dimensional partial differential equations using deep learning. *Proceedings of the National Academy of Sciences*, 115(34):8505–8510.

Han, J. and Long, J. (2020). Convergence of the deep BSDE method for coupled FBSDEs. *Probability, Uncertainty and Quantitative Risk*, 5(1):5.

Harris, F. W. (1990). How many parts to make at once. *Operations Research*, 38(6):947–950.

Harrison, J. M., Sellke, T. M., and Taylor, A. J. (1983). Impulse control of brownian motion. *Mathematics of Operations Research*, 8(3):454–466.

He, K., Zhang, X., Ren, S., and Sun, J. (2015). Delving deep into rectifiers: Surpassing human-level performance on imagenet classification. In *Proceedings of the IEEE international conference on computer vision*, pages 1026–1034.

Helmes, K. L., Stockbridge, R. H., and Zhu, C. (2017). Continuous inventory models of diffusion type: Long-term average costs criterion. *The Annals of Applied Probability*, 27(3):1831–1885.

Huré, C., Pham, H., and Warin, X. (2020). Deep backward schemes for high-dimensional nonlinear pdes. *Mathematics of Computation*, 89(324):1547–1579.

Ignall, E. (1969). Optimal continuous review policies for two product inventory systems with joint setup costs. *Management Science*, 15(5):278–283.

Innes, M. (2018). Flux: Elegant machine learning with Julia. *Journal of Open Source Software*.

Jackson, P., Maxwell, W., and Muckstadt, J. (1985). The joint replenishment problem with a powers-of-two restriction. *IIE Transactions*, 17(1):25–32.

Johnson, E. L. (1967). Optimality and computation of (σ, S) policies in the multi-item infinite horizon inventory problem. *Management Science*, 13(7):475–491.

Kalin, D. (1980). On the optimality of (σ, S) policies. *Mathematics of Operations Research*, 5(2):293–307.

Kaspi, M. and Rosenblatt, M. J. (1991). On the economic ordering quantity for jointly replenished items. *The International Journal of Production Research*, 29(1):107–114.

Kharroubi, I., Ma, J., Pham, H., and Zhang, J. (2010). Backward SDEs with constrained jumps and quasi-variational inequalities. *The Annals of Probability*, 38:797–840.

Khoudja, M. and Goyal, S. (2008). A review of the joint replenishment problem literature: 1989–2005. *European Journal of Operational Research*, 186(1):1–16.

Li, Y. and Sethi, S. (2022). Optimal ordering policy for two product inventory models with fixed ordering costs. Available at SSRN 4199040.

Liu, H. (2004). Optimal consumption and investment with transaction costs and multiple risky assets. *The Journal of Finance*, 59(1):289–338.

Nahmias, S. and Smith, S. A. (1994). Optimizing inventory levels in a two-echelon retailer system with partial lost sales. *Management Science*, 40(5):582–596.

Nocedal, J. and Wright, S. J. (2006). *Numerical Optimization*. Springer.

Øksendal, B. and Sulem, A. (2019). *Stochastic Control of Jump Diffusions*. Springer.

Pantumsinchai, P. (1992). A comparison of three joint ordering inventory policies. *Decision Sciences*, 23(1):111–127.

Perera, S. C. and Sethi, S. P. (2023a). A survey of stochastic inventory models with fixed costs: Optimality of (s, S) and (s, S) -type policies—Continuous-time case. *Production and Operations Management*, 32(1):154–169.

Perera, S. C. and Sethi, S. P. (2023b). A survey of stochastic inventory models with fixed costs: Optimality of (s, S) and (s, S) -type policies—Discrete-time case. *Production and Operations Management*, 32(1):131–153.

Pham, H., Warin, X., and Germain, M. (2021). Neural networks-based backward scheme for fully nonlinear PDEs. *SN Partial Differential Equations and Applications*, 2(1):16.

Porteus, E. L. (1971). On the optimality of generalized (s, S) policies. *Management Science*, 17(7):411–426.

Roundy, R. (1985). 98%-effective integer-ratio lot-sizing for one-warehouse multi-retailer systems. *Management Science*, 31(11):1416–1430.

Roundy, R. (1986). A 98%-effective lot-sizing rule for a multi-product, multi-stage production/inventory system. *Mathematics of Operations Research*, 11(4):699–727.

Scarf, H. (1960). The optimality of (S, s) policies in dynamic inventory problems. In *Mathematical Methods in Social Sciences*, pages 196–202.

Schäl, M. (1976). On the optimality of (s, S) -policies in dynamic inventory models with finite horizon. *SIAM Journal on Applied Mathematics*, 30(3):528–537.

Silver, E. A. (1965). Some characteristics of a special joint-order inventory model. *Operations Research*, 13(2):319–322.

Silver, E. A. (1981). Establishing reorder points in the (S, c, s) coordinated control system under compound Poisson demand. *The International Journal of Production Research*, 19(6):743–750.

Stokey, N. L. (2008). *The Economics of Inaction: Stochastic Control models with fixed costs*. Princeton University Press.

Sulem, A. (1986). A solvable one-dimensional model of a diffusion inventory system. *Mathematics of Operations Research*, 11(1):125–133.

Touzi, N. (2012). *Optimal Stochastic Control, Stochastic Target Problems, and Backward SDE*, volume 29. Springer Science & Business Media.

Veinott Jr, A. F. and Wagner, H. M. (1965). Computing optimal (s, S) inventory policies. *Management Science*, 11(5):525–552.

Viswanathan, S. (1996). A new optimal algorithm for the joint replenishment problem. *Journal of the Operational Research Society*, 47(7):936–944.

Viswanathan, S. (1997). Note. Periodic review (s, S) policies for joint replenishment inventory systems. *Management Science*, 43(10):1447–1454.

Yong, J. and Zhou, X. Y. (1999). *Stochastic Controls: Hamiltonian Systems and HJB Equations*, volume 43. Springer Science & Business Media.

Zheng, Y.-S. and Federgruen, A. (1991). Finding optimal (s, S) policies is about as simple as evaluating a single policy. *Operations Research*, 39(4):654–665.

A. Formal Derivation of Stochastic Identity (15)

Recall the value function V defined in Eq. (11). V is a formal solution to the HJB equation (12). Let $T > 0$, and let $U(\cdot; \alpha, \lambda, \Phi)$ be a reference policy defined by Eq. (13) in Section 4. Also recall the corresponding reference process $\tilde{X}(\cdot)$ given by (14):

$$\tilde{X}(t) = x - \mu t - \sigma B(t) + \sum_{j:T_j \leq t} Y_j.$$

Formally applying a generalized Itô's lemma for jump diffusion to the function $(x, t) \mapsto e^{-rt}V(x)$ (see, e.g., Applebaum (2009)), we have

$$\begin{aligned} e^{-rT}V(\tilde{X}(T)) - V(x) &= \int_0^T e^{-rt}(-rV - \mathcal{L}V)(\tilde{X}(t-))dt - \int_0^T e^{-rt}\nabla V(\tilde{X}(t-))^\top \sigma dB(t) \\ &\quad + \sum_{j:T_j \leq T} e^{-rT_j} [V(\tilde{X}(T_j)) - V(\tilde{X}(T_j-))]. \end{aligned} \quad (26)$$

Then

$$\begin{aligned} V(x) &= e^{-rT}V(\tilde{X}(T)) - \int_0^T e^{-rt}(-rV - \mathcal{L}V)(\tilde{X}(t-))dt + \int_0^T e^{-rt}\nabla V(\tilde{X}(t-))^\top \sigma dB(t) \\ &\quad - \sum_{j:T_j \leq T} e^{-rT_j} [V(\tilde{X}(T_j)) - V(\tilde{X}(T_j-))] \\ &= e^{-rT}V(\tilde{X}(T)) + \int_0^T e^{-rt}[(\mathcal{L} + r)V - f](\tilde{X}(t-))dt + \int_0^T e^{-rt}f(\tilde{X}(t-))dt \\ &\quad + \int_0^T e^{-rt}\nabla V(\tilde{X}(t-))^\top \sigma dB(t) \\ &\quad - \sum_{j:T_j \leq T} e^{-rT_j} [V(\tilde{X}(T_j-) + Y_j) + c(Y_j) - V(\tilde{X}(T_j-))] + \sum_{j:T_j \leq T} e^{-rT_j}c(Y_j) \\ &= e^{-rT}V(\tilde{X}(T)) + \int_0^T e^{-rt}f(\tilde{X}(t-))dt + \int_0^T e^{-rt}\nabla V(\tilde{X}(t-))^\top \sigma dB(t) + \sum_{j:T_j \leq T} e^{-rT_j}c(Y_j) \\ &\quad + \int_0^T e^{-rt}[(\mathcal{L} + r)V - f](\tilde{X}(t-))dt + \sum_{j:T_j \leq T} e^{-rT_j} [V(\tilde{X}(T_j-)) - (V(\tilde{X}(T_j-) + Y_j) + c(Y_j))]. \end{aligned} \quad (27)$$

Consider the two terms in the last line of (27). For notational convenience, write

$$A(\tilde{X}) := \int_0^T e^{-rt}[(\mathcal{L} + r)V - f](\tilde{X}(t-))dt,$$

and

$$B(\tilde{X}) := \sum_{j:T_j \leq T} e^{-rT_j} [V(\tilde{X}(T_j-)) - (V(\tilde{X}(T_j-) + Y_j) + c(Y_j))],$$

where we include the argument \tilde{X} to emphasize the dependence of A and B on the reference process \tilde{X} . The following lemma provides a tight characterization of identity (15) in terms of A and B .

LEMMA 1. *Let $x \in \mathbb{R}^d$. Suppose (27) holds a.s. Then, the stochastic identity (15) holds if and only if the following is true:*

- (i) $A(\tilde{X}) + B(\tilde{X}) \leq 0$ a.s.; and
- (ii) for any $w > 0$, $\mathbb{P}(A(\tilde{X}) + B(\tilde{X}) > -w) > 0$.

We defer the proof of Lemma 1 to the end of the section, and provide a heuristic argument about why both (i) and (ii) should hold, justifying the stochastic identity (15). First, from the HJB equation (12), we have

$$(\mathcal{L} + r)V(x) - f(x) \leq 0, \quad x \in \mathbb{R}^d,$$

implying that $A(\tilde{X}) \leq 0$ a.s. We also have

$$V(x) - \inf_{y \in \mathbb{R}_+^d} (V(x + y) + c(y)) \leq 0, \quad x \in \mathbb{R}^d,$$

implying that for any $Y_j \in \mathbb{R}_+^d$, a.s.,

$$V(x) - (V(x + Y_j) + c(Y_j)) \leq V(x) - \inf_{y \in \mathbb{R}_+^d} (V(x + y) + c(y)) \leq 0,$$

which in turn implies that $B(\tilde{X}) \leq 0$. Thus, $A(\tilde{X}) + B(\tilde{X}) \leq 0$ a.s., establishing (i).

Next, to see why we expect (ii) to be true, consider $A(X^*) + B(X^*)$ where X^* is the state process under an optimal control (which we suppose exists). Then we claim that $A(X^*) = B(X^*) = 0$ a.s. Indeed, under an optimal control, because all ordering decisions are optimal, $B(X^*) = 0$ a.s. Furthermore, we expect $X^*(t)$ to stay within the (closure of) the no-action region for all $t > 0$, with a possible jump into the no-action region at time 0. Thus, the no-action term in (12) is zero for all $t > 0$, a.s., implying that $A(X^*) = 0$ a.s.

Given that $A(X^*) = 0$ and $B(X^*) = 0$ a.s., we wish to show that $\mathbb{P}(A(\tilde{X}) + B(\tilde{X}) > -w) > 0$ for any $w > 0$. To achieve this, one can construct a sequence of processes, starting with the reference process \tilde{X} , that increasingly favors the optimal state trajectories, using a change-of-measure argument. Complete and rigorous treatments can be found in Bouchard (2009) and Kharroubi et al. (2010).

Proof of Lemma 1. Let

$$\begin{aligned} S := \left\{ v \in \mathbb{R} : v - \int_0^T e^{-rt} \nabla V(\tilde{X}(t))^\top \sigma dB(t) \right. \\ \left. \leq e^{-rT} V(\tilde{X}(T)) + \int_0^T e^{-rt} f(\tilde{X}(t)) dt + \sum_{j: T_j \leq T} c(Y_j) e^{-rT_j} \right\} \end{aligned}$$

Then, identity (15) is equivalent to $V(x) = \sup S$. We will show that

$$A(\tilde{X}) + B(\tilde{X}) \leq 0 \text{ a.s.} \iff V(x) \leq \sup S; \text{ and}$$

$$\mathbb{P}(A(\tilde{X}) + B(\tilde{X}) > -w) > 0 \ \forall w > 0 \iff V(x) \geq \sup S,$$

which would complete the proof of the lemma.

First, $A + B \leq 0$ a.s. $\iff \forall \epsilon > 0, A + B \leq \epsilon$ a.s. $\iff \forall \epsilon > 0, V(x) - \epsilon \in S \iff V(x) \leq \sup S$.
Next, $\mathbb{P}(A + B > -w) > 0, \forall w > 0 \iff \forall w > 0, V(x) + w \notin S \iff V(x) \geq \sup S$. \square

B. Implementation Details

B.1. Materials and Method Modifications

We implement two deep neural networks, $H(\cdot; \theta)$ and $G(\cdot; \theta)$, both consisting of two to four (hidden) layers. The neural networks are implemented using the `Flux.jl` package (Innes, 2018) in the `Julia 1.10` computing language (Bezanson et al., 2017). Currently, we conduct the numerical experiments on a high-performance computing node equipped with an NVIDIA H100 GPU with 80 GB memory and an AMD EPYC 9334 32-core processor, allowing up to 64 logical threads, with 694 GB of usable RAM.

Neural network architecture. As mentioned, our neural networks are fully connected with two to four hidden layers, using `elu` activation functions at the nodes. We initialize the weights with random numbers drawn from a uniform distribution using Kaiming (He) initialization (He et al., 2015).

Data generation. The time horizon T is tuned for each test problem, and we choose the number of time intervals N large enough so that the time step satisfies $\Delta t \leq 0.005$, which our empirical tests indicate is sufficient for accurate results. The batch size refers to the number of sample paths generated. The number of iterations equals the number of epochs, as for each iteration, the entire data set, i.e., output from Subroutine 1 over all sample paths in the batch, is generated and used during training. See tables in Section B.2 below for more details.

Reference policy parameters. We choose ν and α via extensive hyperparameter tuning. We set λ to the average ordering rate of the (R, S) policy when using the (Q, S) policy’s S vector as the reference (i.e., set $\mathbb{E}[Z] = S$). Otherwise, if we pick can-order’s S vector as reference, we set λ to the can-order policy’s average annual ordering rate.

NN optimizer. The neural network parameters and corresponding gradients are updated using the `Adam` optimizer. The learning rates and penalties $\{\beta_m\}_{m=1}^M$ follow step-based updating schemes. Both schemes, for the different test problems, are outlined in the tables below.

Cost scaling. It is easy to show, under the assumed cost structure, that the impulse-control problem is invariant under any positive scaling of the cost parameters. For $\kappa > 0$, consider scaled costs $\kappa c_0, \kappa c, \kappa h, \kappa p$. Then, by linearity, the inventory-state cost is $\kappa f(x)$ and the ordering cost is $\kappa c(y)$. For any admissible policy u ,

$$V_\kappa(x, u) = \mathbb{E}_x \left[\int_0^\infty e^{-rt} \kappa f(X^u(t)) dt + \sum_j e^{-r\tau_j} \kappa c(y^{(j)}) \right] = \kappa V(x, u).$$

Hence

$$V_\kappa(x) = \inf_{u \in \mathcal{U}} V_\kappa(x, u) = \inf_{u \in \mathcal{U}} \kappa V(x, u) = \kappa \inf_{u \in \mathcal{U}} V(x, u) = \kappa V(x).$$

Thus, scaling all costs by κ multiplies the value function by κ , and allows us to use cost rescaling during neural network training for the sake of numerical stability, without loss of generality.

Numerical optimizer. To compute our policy’s reorder level z^* , we use one of two approaches. The first approach is to solve the minimization problem in Eq. (22). For this, we use the L-BFGS implementation (Nocedal and Wright, 2006) in `Optim.jl`. Since the neural network approximations are reliable only in regions of the state space that were sufficiently explored during training, we impose box constraints to confine the search for z^* to a domain we expect has been learned well. We implement these constraints by wrapping the L-BFGS optimization routine in `Fminbox` (Dixit and Rackauckas, 2023). We use the bounds and initial points listed in Appendix B.2. The alternative is to use the stationarity condition in Eq. (25), and find a stationary point by minimizing the least-squares objective $\inf_z \frac{1}{2} \|G_\vartheta(z) + c\|_2^2$, again with L-BFGS.

B.2. Hyperparameter Configurations

Table 8: Common hyperparameter configurations for neural network training outlined per group of test problems (the final penalty rate, β_{final} , is tuned for each test problem separately; see Tables 10 - 13 for details).

Hyperparameter	2-Dimensional	12-D (Low & Medium CV)	12-D (High CV)	50-Dimensional
Number of hidden layers	4	3	3	3
Neurons per layer	500	1,000	1,000	1,000
Activation function	elu	elu	elu	elu
Batch size (K)	2,500	5,000	5,000	5,000
Time intervals (N)	50	50	50	50
Number of iterations	25,000	40,000	40,000	40,000
Scaling κ	0.1	0.1	0.1	0.01
Learning rate (iteration range)	10^{-3} (1–10,000)	10^{-3} (1–5,000)	10^{-3} (1–5,000)	10^{-3} (1–5,000)
	10^{-4} (10,000–15,000)	$5 \cdot 10^{-4}$ (5,000–10,000)	$2 \cdot 10^{-4}$ (5,000–10,000)	$2 \cdot 10^{-4}$ (5,000–10,000)
	10^{-5} (15,000–20,000)	10^{-4} (10,000–15,000)	10^{-4} (10,000–20,000)	10^{-4} (10,000–20,000)
	10^{-6} (20,000–25,000)	10^{-5} (15,000–20,000)	10^{-5} (20,000–30,000)	10^{-5} (20,000–30,000)
Penalty rate (iteration range)	10^0 (1–2,500)	10^0 (1–2,500)	10^0 (1–2,500)	10^0 (1–2,500)
	10^1 (2,500–5,000)	10^1 (2,500–5,000)	10^1 (2,500–5,000)	10^1 (2,500–5,000)
	10^2 (5,000–7,500)	10^2 (5,000–7,500)	10^2 (5,000–7,500)	10^2 (5,000–7,500)
	10^3 (7,500–10,000)	10^3 (7,500–10,000)	10^3 (7,500–10,000)	10^3 (7,500–10,000)
	10^4 (10,000–15,000)	10^4 (10,000–15,000)	10^4 (10,000–20,000)	10^4 (10,000–20,000)
	10^5 (15,000–20,000)	10^5 (15,000–20,000)	β_{final} (20,000–40,000)	β_{final} (20,000–40,000)
	10^6 (20,000–40,000)	β_{final} (20,000–40,000)		

Table 9: Problem-specific hyperparameters for 2-dimensional test problems ($\mathbb{E}[Z]$ is chosen as a nearby value of the MDP solution; bounds and initial points are scaled by $\mathbb{E}[Z]$ componentwise).

Test Instance	T	λ	ν	α	Φ	$\mathbb{E}[Z]$	ϵ	Opt. Method	Opt. Bounds	Opt. Start
Base Case	0.1	1.0	0.2	0	Lognormal	$[35, 20]^\top$	-2.5	Solve Eq. (22)	[0.0, 1.5]	1.0
Low CV	0.1	1.0	0.2	0	Lognormal	$[35, 20]^\top$	-2.5	Solve Eq. (22)	[0.0, 1.5]	1.0
High CV	0.1	1.0	0.4	0	Lognormal	$[30, 20]^\top$	-5.0	Solve Eq. (22)	[0.0, 1.5]	1.0
$c_0 = 20$	0.1	1.0	0.2	0	Lognormal	$[20, 15]^\top$	-2.5	Solve Eq. (22)	[0.0, 1.5]	1.0
$c_0 = 100$	0.1	1.0	0.2	0	Lognormal	$[50, 30]^\top$	-5.0	Solve Eq. (22)	[0.0, 1.5]	1.0
$p = 10$	0.1	1.0	0.2	0	Lognormal	$[30, 20]^\top$	-2.5	Solve Eq. (22)	[0.0, 1.5]	1.0
$p = 100$	0.1	1.0	0.2	0	Lognormal	$[35, 20]^\top$	-5.0	Solve Eq. (22)	[0.0, 1.5]	1.0

Table 10: Problem-specific hyperparameters for 12-dimensional test problems with Poisson demand ($\mathbb{E}[Z]$ is set to the S vector of one of the benchmark policies; bounds and initial points are scaled by $\mathbb{E}[Z]$ componentwise).

c_0	p	T	λ	ν	α	β_{final}	Φ	$\mathbb{E}[Z]$	ϵ	Opt. Method	Opt. Bounds	Opt. Start
20	10	0.1	4.00	0.2	0.4	10^6	Lognormal	(Q, S)	-2.5	Eq. (22)	[0.0, 2.0]	0.5
		0.1	4.73	0.1	0.0	10^6	Lognormal	(Q, S)	-5.0	Eq. (22)	[0.0, 2.0]	0.5
		0.1	4.73	0.2	0.2	10^6	Lognormal	(Q, S)	-2.5	Eq. (22)	[0.0, 2.0]	0.5
100	10	0.1	1.73	0.1	0.0	10^6	Lognormal	(Q, S)	-7.5	Eq. (22)	[0.0, 2.0]	0.5
		0.1	2.08	0.2	0.2	10^6	Lognormal	(Q, S)	-10.0	Eq. (22)	[0.0, 2.0]	0.5
		0.1	2.08	0.1	0.0	10^6	Lognormal	(Q, S)	-12.5	Eq. (22)	[0.0, 2.0]	0.5
200	10	0.1	1.21	0.2	0.2	10^6	Lognormal	(Q, S)	-10.0	Eq. (22)	[0.0, 2.0]	0.5
		0.1	1.37	0.4	0.0	10^6	Lognormal	(Q, S)	-30.0	Eq. (25)	[0.5, 1.5]	1.0
		0.1	1.41	0.4	0.0	10^6	Lognormal	(Q, S)	-40.0	Eq. (25)	[0.5, 1.5]	1.0

Table 11: Problem-specific hyperparameters for 12-dimensional test problems with negative binomial demand (CV=0.5) ($\mathbb{E}[Z]$ is set to the S vector of one of the benchmark policies; bounds and initial points are scaled by $\mathbb{E}[Z]$ componentwise).

c_0	p	T	λ	ν	α	β_{final}	Φ	$\mathbb{E}[Z]$	ϵ	Opt. Method	Opt. Bounds	Opt. Start
20	10	0.1	5.78	0.2	0.0	10^6	Lognormal	(Q, S)	-12.5	Eq. (22)	[0.0, 2.0]	0.5
	50	0.1	7.43	0.4	0.4	10^6	Lognormal	(Q, S)	-7.5	Eq. (22)	[0.0, 2.0]	0.5
	100	0.1	7.43	0.2	0.2	10^6	Lognormal	(Q, S)	-2.5	Eq. (22)	[0.0, 2.0]	0.5
100	10	0.1	2.08	0.8	0.0	10^6	Lognormal	(Q, S)	-30.0	Eq. (25)	[0.5, 1.5]	1.0
	50	0.1	2.48	0.2	0.4	10^6	Lognormal	(Q, S)	-25.0	Eq. (22)	[0.0, 2.0]	0.5
	100	0.1	2.74	0.2	0.4	10^6	Lognormal	(Q, S)	-50.0	Eq. (22)	[0.0, 2.0]	0.5
200	10	0.1	1.37	0.2	0.2	10^6	Lognormal	(Q, S)	-25.0	Eq. (22)	[0.0, 2.0]	0.5
	50	0.1	1.73	0.2	0.4	10^6	Lognormal	(Q, S)	-50.0	Eq. (22)	[0.0, 2.0]	0.5
	100	0.1	1.79	0.2	0.4	10^6	Lognormal	(Q, S)	-50.0	Eq. (22)	[0.0, 2.0]	0.5

Table 12: Problem-specific hyperparameters for 12-dimensional test problems with negative binomial demand (CV=1.0) ($\mathbb{E}[Z]$ is set to the S vector of one of the benchmark policies; bounds and initial points are scaled by $\mathbb{E}[Z]$ componentwise).

c_0	p	T	λ	ν	α	β_{final}	Φ	$\mathbb{E}[Z]$	ϵ	Opt. Method	Opt. Bounds	Opt. Start
20	10	0.05	8.67	0.4	0.0	10^6	Lognormal	(Q, S)	-7.5	Eq. (22)	[0.75, 1.25]	1.0
	50	0.05	9.53	0.05	0.2	10^5	Lognormal	Can-Order	-7.5	Eq. (22)	[0.5, 1.5]	1.0
	100	0.05	6.95	0.1	0.4	10^5	Lognormal	Can-Order	-1.25	Eq. (22)	[0.5, 1.5]	1.0
100	10	0.05	3.25	0.8	0.4	10^7	Lognormal	(Q, S)	-50.0	Eq. (22)	[0.75, 1.25]	1.0
	50	0.05	3.54	0.8	0.0	10^5	Lognormal	Can-Order	-50.0	Eq. (22)	[0.5, 1.5]	1.0
	100	0.05	3.60	1.2	0.0	10^5	Lognormal	Can-Order	-2.5	Eq. (25)	[0.5, 1.5]	1.0
200	10	0.1	1.93	0.4	0.4	10^7	Lognormal	(Q, S)	-100.0	Eq. (22)	[0.75, 1.25]	1.0
	50	0.05	2.79	0.8	0.2	10^5	Lognormal	Can-Order	-50.0	Eq. (22)	[0.5, 1.5]	1.0
	100	0.05	2.54	0.8	0.0	10^5	Lognormal	Can-Order	-50.0	Eq. (22)	[0.5, 1.5]	1.0

Table 13: Problem-specific hyperparameters for 50-dimensional test problems ($\mathbb{E}[Z]$ is set to the S vector of one of the benchmark policies; bounds and initial points are scaled by $\mathbb{E}[Z]$ componentwise).

c_0	Demand CV	T	λ	ν	α	β_{final}	Φ	$\mathbb{E}[Z]$	ϵ	Opt. Method	Opt. Bounds	Opt. Start
50	Poisson	0.05	5.78	0.2	0.00	10^5	Lognormal	(Q, S)	-1.25	Eq. (25)	[0.5, 1.5]	1.0
	0.5	0.05	8.67	0.1	0.00	10^6	Lognormal	(Q, S)	-15.0	Eq. (25)	[0.5, 1.5]	1.0
	1.0	0.20	17.33	0.1	0.00	10^5	Lognormal	(Q, S)	-5.0	Eq. (25)	[0.5, 1.5]	1.0
150	Poisson	0.05	3.25	0.05	0.0	10^6	Lognormal	(Q, S)	-5.0	Eq. (25)	[0.5, 1.5]	1.0
	0.5	0.05	4.33	0.1	0.2	10^5	Lognormal	(Q, S)	-10.0	Eq. (25)	[0.5, 1.5]	1.0
	1.0	0.20	8.67	0.2	0.0	10^5	Lognormal	(Q, S)	-5.0	Eq. (25)	[0.5, 1.5]	1.0
250	Poisson	0.05	2.60	0.1	0.0	10^5	Lognormal	(Q, S)	-5.0	Eq. (25)	[0.5, 1.5]	1.0
	0.5	0.05	3.25	0.1	0.2	10^6	Lognormal	(Q, S)	-15.0	Eq. (25)	[0.5, 1.5]	1.0
	1.0	0.2	5.78	0.8	0.0	10^5	Lognormal	(Q, S)	-5.0	Eq. (25)	[0.5, 1.5]	1.0

C. Implementation of Benchmarks

C.1. MDP Benchmarks

To obtain the optimal solution for the two-dimensional test problems, we minimize (4) to obtain the value function $V(x) := \inf_u J(x, u)$, which is known to be characterized by the Bellman equation

$$V(x) = \min_{y \in \mathbb{N}_0^d} \left\{ \sum_{x' \in \mathbb{Z}^d} p(x, x', y) (f(x') + c(y) + \gamma V(x')) \right\}, \quad (28)$$

where $f(x')$ is the per-period inventory cost when the end-of-period inventory is x' , and $p(x, x', y)$ is the probability of moving from inventory state x to x' given order vector y , determined by the underlying demand distribution.

It is computationally feasible to solve the two-dimensional problems using standard MDP techniques, yielding the benchmarks to which we compare our proposed policy derived from the continuous-time impulse control formulation. To be specific, we solve (28) using policy iteration (see, e.g., Bertsekas, 2012, Section 2.3).

To achieve such computational feasibility, it is necessary to truncate the state and action spaces. The following propositions formally justify that we can perform these truncations.

PROPOSITION 1. *The minimization in (28) over order quantities $y \in \mathbb{N}_0^d$ is equivalent to a minimization over order-up-to levels $z \in \mathbb{Z}^d$ with $z \geq x$ componentwise.*

Proof. Let us denote the state after ordering by $z = x + y$. Since $y \geq 0$, it must hold that $z \geq x$. We can then perform a change of variables in the Bellman equation from y to z . The action space becomes choosing an order-up-to level $z \in \{z' \in \mathbb{Z}^d : z' \geq x\}$. The Bellman equation is then rewritten as

$$V(x) = \min_{z \geq x} \{c(z - x) + \gamma \mathbb{E}[f(z - \xi) + V(z - \xi)]\}. \quad (29)$$

It is easily verified that there exists a one-to-one mapping between any feasible order quantity y and an order-up-to level z for each inventory state x . Therefore, the minimization problems in (28) and (29) are equivalent. Thus, restricting the search to order-up-to policies can be done without loss of optimality. \square

Proposition 1 yields an alternative Bellman equation that we can solve using policy iteration. Recall that Johnson (1967) characterizes the optimal policy as the (σ, S) policy described earlier. This implies that if the initial state $x \leq S$ componentwise, then one orders up to the vector S thereafter, since demand is nonnegative. Under mild assumptions on the cost parameters (e.g., backlogging costs substantially exceed holding costs), the order-up-to vector is known to be positive. In our numerical experiments, we set the initial state to $x = 0$, so a single optimal vector S exists. The following proposition is essentially an immediate corollary of the results in Johnson (1967), and greatly simplifies the search for the optimal solution.

PROPOSITION 2. *Suppose that demand is nonnegative, the optimal order-up-to vector S^* is nonnegative, and the initial inventory state x satisfies $x_i \leq S_i$ for each item i . Then, there exists a bounded set $\mathcal{Z} \subset \mathbb{N}_0^d$ such that an optimal order-up-to policy orders up to $S^* \in \mathcal{Z}$. Moreover, the state space can be truncated without loss of optimality.*

Proof. Under the stated assumptions, it follows from the results in Johnson (1967) that under the optimal policy, inventory is raised to a single order-up-to vector S^* (independent of x). It is easily verified that the unbounded increase in costs for large z ensures that the optimal order-up-to level, S^* , which minimizes the total cost, must be finite. Note further from our assumptions, that we can lower bound z by zero. Therefore, we can restrict the search for S^* to a sufficiently large compact set $\mathcal{Z} = \{z \in \mathbb{Z}^d : \underline{z}_i \leq z_i \leq \bar{z}_i, i = 1, \dots, d\}$ without loss of optimality.

Restricting the action space allows for the truncation of the state space. Under any order-up-to policy with $z \in \mathcal{Z}$, the inventory level immediately after replenishment is $z \in \mathcal{Z}$, so that $x_i \leq \bar{z}_i$. Since demand is nonnegative, the inventory level for item i never exceeds \bar{z}_i . This means that states where $x_i > \bar{z}_i$ are not reachable under such a policy. It is therefore sufficient to solve the MDP on a truncated state space $\mathcal{X} := \{x \in \mathbb{Z}^d : x_i \leq \bar{x}_i, i = 1, \dots, d\}$, provided the upper bound \bar{x} is chosen to be at least as large as the upper bound \bar{z} of the optimal action space. \square

In our two-dimensional test problems, we truncate the action space by considering only order-up-to levels $z \in [0, 100]^2$. These bounds were chosen via preliminary computations with the other benchmark policies so that we could identify a region where the optimal policy is likely to operate. The state space is similarly restricted by setting the lower and upper bounds to -200 and 100, respectively.

C.2. Benchmark Policies

In this section, we describe in detail the benchmark policies that we use for performance comparisons. We evaluate the performances of the benchmark policies under the expected total discounted cost criterion, with the annual interest rate being set to $r = 0.05$. In all our experiments, the initial inventory levels are set to 0 for all items.

All benchmark policies described here are each defined by a set of parameters. To determine these parameters, we are often required to consider inventory problems that are related but different from the original SJRP. For example, to set the parameters s and S for independent (s, S) policies, we consider several single-item inventory problems. For these related inventory problems, we use the same annual interest rate of $r = 0.05$, and the expected total discounted cost objective. We first discuss the independent (s, S) policy, and then review the (R, S) , (Q, S) and can-order policies.

Independent (s, S) policies. An independent (s, S) policy computes a reorder point s_i and an order-up-to level S_i for item i , $i = 1, \dots, d$. Whenever the inventory level of item i drops to or below s_i , the policy places an order to bring the i th inventory level to S_i . In other words, the policy performs independent replenishment for each item, without considering the opportunities for cost savings through coordinated replenishment.

We consider a parametrized family of independent (s, S) policies, parametrized by $\alpha \in (0, 1]$. For a given $\alpha \in (0, 1]$, the corresponding independent (s, S) policy determines the reorder points s_i and

the order-up-to level S_i as follows. For $i = 1, 2, \dots, d$, s_i and S_i correspond to the optimal reorder point and order-up-to level, respectively, of a one-item inventory model involving only item i , with demand process D_i defined in Eq. (8), unit holding cost h_i , unit backlogging cost p_i , unit variable cost c_i , and fixed ordering cost αc_0 . In other words, the independent (s, S) policies differ only in the fixed cost used to determine the s_i and S_i levels.

When $\alpha = 1$, we call the corresponding policy the vanilla independent (s, S) policy. The vanilla policy is a common and natural benchmark used in the literature (see, e.g., Atkins and Iyogun, 1988; Viswanathan, 1997). We consider a larger family of policies, as α ranges in $(0, 1]$, to potentially improve performance over the vanilla policy. Policies with different α achieve different tradeoffs between the inventory related costs (i.e., holding and backlogging costs) and the fixed ordering costs. Indeed, an independent (s, S) policy with a smaller α places more frequent orders, thereby reducing inventory related costs and increasing the ordering costs. Computationally, the parameters s_i and S_i are determined using the approach in Zheng and Federgruen (1991).

We simulate the performances of independent (s, S) policies with α taking values in the set $\{0.05, 0.1, \dots, 1\}$, and report the one with the lowest expected total discounted cost. For each performance evaluation, we generate 10,000 sample paths, each run for 10,000 periods. Given an annual interest rate of $r = 0.05$, the discount factor at termination is less than $\exp(-r \cdot 10000/52) \approx 7 \times 10^{-5}$, indicating a negligible error resulting from truncation of the time horizon.

Periodic review (R, S) policy. A periodic review (R, S) policy is specified by $d+1$ parameters: the review period R , and for item i , $i = 1, \dots, d$, the base-stock level S_i . Starting at the beginning of the first week, an order is placed every R weeks, which brings the inventory level of item i to S_i , $i = 1, \dots, d$. Let us note that even though a negative basestock level is theoretically possible under certain parameter regimes—for example, when the backlogging cost is much smaller than the holding cost—we do not consider this case and restrict our attention to nonnegative basestock levels. Indeed, in all our numerical experiments, backlogging costs are substantially larger than holding costs, as is often the case in practice, so we expect that (R, S) policies with $S \in \mathbb{R}_+^d$ to perform competitively.

We now explain and describe a computationally efficient procedure to determine the best (R, S) policy. We begin by deriving explicit expressions for the expected total discounted fixed cost of ordering and sum of holding, backlogging, and variable ordering costs.

PROPOSITION 3. *Under a given (R, S) policy, with $S \geq 0$ component-wise:*

(a) *If $S = 0$, the expected total discounted fixed cost of ordering is*

$$c_0 \mathbb{P} \left(\sum_{i=1}^d D_i^{(R)} > 0 \right) (\gamma^R + \gamma^{2R} + \dots) = \frac{c_0 \gamma^R}{1 - \gamma^R} \mathbb{P} \left(\sum_{i=1}^d D_i^{(R)} > 0 \right), \quad (30)$$

where c_0 is fixed ordering cost, γ is the weekly discount factor, and for $i = 1, 2, \dots, d$ and $r = 1, 2, \dots, R$, $D_i^{(r)}$ has the same distribution as the cumulative demand for item i over r weeks.

If there exists i such that $S_i > 0$, the expected total discounted fixed cost of ordering is

$$c_0 + \frac{c_0 \gamma^R}{1 - \gamma^R} \mathbb{P} \left(\sum_{i=1}^d D_i^{(R)} > 0 \right), \quad (31)$$

(b) *For item i , the expected total discounted holding, backlogging and variable ordering cost is given by*

$$c_i S_i + \frac{1}{1 - \gamma^R} \sum_{r=0}^{R-1} \gamma^r \mathbb{E} \left[f_i \left(S_i - D_i^{(r+1)} \right) \right] + \frac{1}{1 - \gamma^R} \cdot c_i \mathbb{E} \left[D_i^{(R)} \right], \quad (32)$$

where γ and $D_i(r)$ are as before, c_i is the unit variable cost for item i , and $f_i(\cdot)$ is the inventory cost function defined in Eq. (1).

Proof. We first prove part (a). Consider a (R, S) policy with $S = 0$ component-wise. Then, no order is placed at time 0. From time 0 to the beginning of week R , item- i inventory is reduced by an amount distributed exactly as $D_i^{(R)}$, $i = 1, 2, \dots, d$. If the total inventory consumed during this time is positive, which happens with probability $\mathbb{P} \left(\sum_{i=1}^d D_i^{(R)} > 0 \right)$, an order is placed at the beginning of week R , incurring a discounted fixed cost of $c_0 \gamma^R$. Thus, the expected discounted fixed cost of ordering incurred is $\mathbb{P} \left(\sum_{i=1}^d D_i^{(R)} > 0 \right) c_0 \gamma^R$. Similarly, the expected discounted fixed cost of ordering incurred at time $2R$ is $\mathbb{P} \left(\sum_{i=1}^d D_i^{(R)} > 0 \right) c_0 \gamma^{2R}$, and so on and so forth. Summing up the expected discounted fixed cost of ordering at times $R, 2R, \dots$ gives the expression (30).

If there exists i such that $S_i > 0$, then an order is placed at time 0, incurring an additional cost of c_0 . The subsequent expected discounted fixed costs of ordering incurred at times $R, 2R, \dots$ are exactly the same as in the case with $S = 0$. Thus, the expected total discounted fixed cost of ordering in this case is the sum of c_0 and expression (30), giving the expression (31).

Next, we prove part (b). For item i , the discounted variable cost incurred at time 0 is $c_i S_i$, and that incurred at time kR has distribution $\gamma^{kR} c_i D_i^{(R)}$, $k = 1, 2, \dots$. Thus, the expected total discounted variable cost of ordering is

$$c_i S_i + \sum_{k=1}^{\infty} \gamma^{kR} c_i \mathbb{E} [D_i^{(R)}] = c_i S_i + \frac{\gamma^R}{1 - \gamma^R} \cdot c_i \mathbb{E} [D_i^{(R)}].$$

The discounted holding and backlogging cost incurred at time $kR+r$, where $r = 0, 1, \dots, R-1$, $k = 0, 1, 2, \dots$, has distribution $\gamma^{kR+r} f_i (S_i - D_i^{(r+1)})$. Summing over all times and taking expectations, we have that the expected total discounted holding and backlogging cost is

$$(1 + \gamma^R + \dots) \sum_{r=0}^{R-1} \gamma^r \mathbb{E} [f_i (S_i - D_i^{(r+1)})] = \frac{1}{1 - \gamma^R} \sum_{r=0}^{R-1} \gamma^r \mathbb{E} [f_i (S_i - D_i^{(r+1)})].$$

Summing up preceding two expected total discounted costs gives the expression (31). \square

Note that expressions (30) and (31) are independent of the levels S_i , and the expression (32) involves only parameters and demand distributions associated with item i , not other items. These properties suggest the following method to find the optimal parameters R^* and S_i^* . First, under a fixed review period R , for each i , we compute the optimal item- i base-stock $S_i^*(R)$ by optimizing the expression (32) over S_i , which becomes

$$S_i^*(R) = \arg \min_{y \geq 0} (1 - \gamma^R) c_i y + \sum_{r=0}^{R-1} \gamma^r \mathbb{E} [f(y - D_i^{(r+1)})]. \quad (33)$$

Next, to find the optimal review period R^* , we simulate the performances of all $(R, S^*(R))$ policies, where $R \in \{1, 2, \dots, R_{\max}\}$, and $S^*(R)$ is the vector of optimal base-stock levels corresponding to review period R . We set $R_{\max} = 100$, roughly 2 years, since we do not expect the best policy to not order for that long (given our current choices for the fixed cost c_0).

(Q, S) policy. Similar to the (R, S) policies, a (Q, S) policy is also specified by $d+1$ parameters: the replenishment coordination parameter Q and a base-stock level S_i for each item $i = 1, \dots, d$. Every time the cumulative aggregate demand since the previous replenishment reaches or exceeds Q , an order is placed to bring the inventory level of item i back to its base-stock level S_i , $i = 1, \dots, d$.

The method for finding the optimal policy parameters for (Q, S) policies is similar to the one for (R, S) policies. We first fix Q and compute the optimal base-stocks $S^*(Q)$, and then simulate performances of $(Q, S^*(Q))$ policies to determine the best Q^* (and associated $S^*(Q^*)$). A major

difference is that a (Q, S) policy involves a random review period, which we denote by R_Q , whereas the review period is deterministic under a (R, S) policy. More specifically, as previously described, R_Q is the number of weeks until the cumulative aggregate demand since the last order reaches or exceeds Q . Thus R_Q has the same distribution as

$$\min \left\{ R \in \mathbb{Z}_+ : \sum_{i=1}^d D_i^{(R)} \geq Q \right\}, \quad (34)$$

where we recall that $D_i^{(r)}$ is the cumulative demand of item i over r weeks.

We next derive an explicit expression for the expected total discounted cost under an arbitrary (Q, S) policy. It follows from recognizing that the system regenerates at each order epoch, and by applying a suitable renewal-theoretic argument.

PROPOSITION 4. *Under a given (Q, S) policy and assuming i.i.d. demand, with $S \geq 0$ componentwise and an order placed at time $t = 0$ to bring the inventory level back to S :*

(a) *If there exists i such that $S_i > 0$, then the expected total discounted fixed cost of ordering is given by*

$$\frac{c_0}{1 - \mathbb{E}[\gamma^{R_Q}]} \cdot \quad (35)$$

(b) *For item i , the total expected discounted holding, backlogging, and variable ordering cost is given by*

$$c_i S_i + \frac{\mathbb{E} \left[\sum_{t=0}^{R_Q-1} \gamma^t f_i(S_i - D_i^{(t+1)}) \right] + c_i \mathbb{E}[\gamma^{R_Q} D_i^{(R_Q)}]}{1 - \mathbb{E}[\gamma^{R_Q}]} \cdot \quad (36)$$

Proof. The proof relies on a renewal-reward expression for discounted costs. Let $J(S)$ be the total expected discounted cost starting from the regenerative inventory state S , which occurs immediately after an order is placed. By definition, this total cost is given by

$$J(S) = \mathbb{E} \left[\sum_{t=0}^{\infty} \gamma^t C_t \right],$$

where C_t denotes all costs that are incurred in period t . We next decompose this sum into the costs incurred during the first cycle and all subsequent costs. That is,

$$J(S) = \mathbb{E} \left[\sum_{t=0}^{R_Q-1} \gamma^t C_t + \sum_{t=R_Q}^{\infty} \gamma^t C_t \right].$$

The first term in the expectation is the total discounted cost within the first cycle, which we denote as $\mathbb{E}[C_{\text{cycle}}]$. For the second term, we can factor out γ^{R_Q} so that

$$\sum_{t=R_Q}^{\infty} \gamma^t C_t = \gamma^{R_Q} \sum_{k=0}^{\infty} \gamma^k C_{R_Q+k}.$$

It is key to note that at time R_Q , the system probabilistically restarts from state S so that from that point forward the total discounted cost is again $J(S)$, regardless of the history that led to the first replenishment. From the law of total expectation and the fact that the replenishment cycles are of an i.i.d. nature, we thus obtain

$$\begin{aligned} J(S) &= \mathbb{E}[C_{\text{cycle}}] + \mathbb{E} \left[\gamma^{R_Q} \left(\sum_{k=0}^{\infty} \gamma^k C_{R_Q+k} \right) \right] \\ &= \mathbb{E}[C_{\text{cycle}}] + \mathbb{E} \left[\mathbb{E} \left[\gamma^{R_Q} \left(\sum_{k=0}^{\infty} \gamma^k C_{R_Q+k} \right) \mid R_Q \right] \right] \\ &= \mathbb{E}[C_{\text{cycle}}] + \mathbb{E}[\gamma^{R_Q}] J(S). \end{aligned}$$

Solving for $J(S)$ then yields

$$J(S) = \frac{\mathbb{E}[C_{\text{cycle}}]}{1 - \mathbb{E}[\gamma^{R_Q}]}.$$

This principle allows us to determine the total expected discounted cost by considering a single replenishment cycle.

(a) Note that we incur the fixed cost c_0 at the beginning of each cycle (i.e., at times $T_0 = 0, T_1 = R_{Q,1}, T_2 = R_{Q,1} + R_{Q,2}$, etc.). We can write the expected present value of this stream of fixed costs as

$$\mathbb{E} \left[\sum_{k=0}^{\infty} \gamma^{T_k} c_0 \right] = c_0 \sum_{k=0}^{\infty} \mathbb{E}[\gamma^{T_k}] = c_0 \sum_{k=0}^{\infty} (\mathbb{E}[\gamma^{R_Q}])^k = \frac{c_0}{1 - \mathbb{E}[\gamma^{R_Q}]},$$

where exchanging the sum and expectation is justified by nonnegativity of the summands, and the second equality uses that the cycle lengths $R_{Q,k}$ are i.i.d.

(b) For item i , the cost consists of the initial order cost and the subsequent costs. The initial variable cost to raise inventory from 0 to S_i is $c_i S_i$. After this, the system is in the regeneration state S . The expected discounted cost over a single cycle for item i , discounted to the start of the cycle, consists of holding/backlogging costs during the cycle and the variable ordering cost at the end of the cycle, and is thus given by

$$\mathbb{E} \left[\sum_{t=0}^{R_Q-1} \gamma^t f_i(S_i - D_i^{(t+1)}) + \gamma^{R_Q} c_i D_i^{(R_Q)} \right].$$

The total expected discounted cost for item i from $t = 0+$ onward is obtained by dividing the single-cycle cost by $1 - \mathbb{E}[\gamma^{R_Q}]$. Adding the initial variable cost yields (36). \square

For the demand distributions that we consider, R_Q may not have simple closed-form distribution functions. However, we can simulate R_Q using the expression (34), and compute the optimal base-stock level $S_i^*(Q)$ by solving

$$S_i^*(Q) = \arg \min_{y \geq 0} \mathbb{E}_{R_Q} \left[(1 - \gamma^{R_Q}) c_i y + \sum_{r=0}^{R_Q-1} \gamma^r \mathbb{E}[f_i(y - D_i^{(r+1)})] \right], \quad (37)$$

for $i = 1, 2, \dots, d$, using simulation-optimization techniques such as sample average approximation. We then simulate the performances of all $(Q, S^*(Q))$ policies, for Q in a judiciously chosen range. To be precise, we look at the associated optimal review period R^* found earlier and then vary Q over $\{(\lfloor (R^* - 5) \sum \mathbb{E}[D_i] \rfloor)^+, (\lfloor (R^* - 5) \sum \mathbb{E}[D_i] \rfloor + 1)^+, \dots, \lfloor (R^* + 5) \sum \mathbb{E}[D_i] \rfloor\}$ in order to find the optimal Q^* .

Can-order policy. A can-order policy is specified by $3d$ parameters, reorder points s_i , can-order points o_i , and order-up-to levels S_i , $i = 1, \dots, d$, with $s_i \leq o_i \leq S_i$ for each i . Whenever the inventory level of some item, say item i , drops to or below s_i , an order is placed. For item i , the order raises its inventory level to S_i . For item j with $j \neq i$, if its inventory level is at or below o_j , the same order replenishes item j to raise the inventory level to S_j .

Finding the best can-order policy involves optimizing over $3d$ parameters *a priori*, which is computationally infeasible for large d . Therefore, we proceed with a heuristic approach, which involves optimization over two parameters, α and κ , both of which take values in $[0, 1]$. The parameter α is used to determine the reorder points s_i and the order-up-to levels S_i , and κ is then used to determine the can-order levels o_i . More specifically, for a given α , we first determine the values of s_i and S_i according to an independent (s, S) policy with parameter α , as previously described. Then, given κ , we set the can-order levels o_i according to

$$o_i = \kappa s_i + (1 - \kappa) S_i, \quad i = 1, \dots, d.$$

We simulate the performances of can-order policies for all pairs (α, κ) in the set $\{0, 0.05, \dots, 1\} \times \{0, 0.1, \dots, 1.0\}$, and report the best performing policy. Each performance evaluation is obtained using 10,000 sample paths, each run for 10,000 periods.

D. Validation of Methodology in 1-Dimensional Setting with Diffusion Demand

To validate our computational method, we consider the single-item inventory control problem discussed in Sulem (1986). The inventory levels are allowed to be continuous. We further assume that inventory levels are continuously reviewed, and cumulative demand follows the Brownian motion

$$D(t) = \mu t + \sigma B(t).$$

We treat the infinite-horizon, continuously discounted costs problem in one dimension. The evolution of the inventory level is described by the one-dimensional stochastic process $X^u(\cdot)$, with

$$X^u(t) = x - D(t) + \sum_{\{j: \tau_j \leq t\}} y_j, \quad (38)$$

where x is the initial inventory level, and y_j is the amount ordered at time τ_j . The goal is to minimize the expected total discounted cost, where costs are continuously discounted over time. Putting this all together, the total expected discounted cost is given by

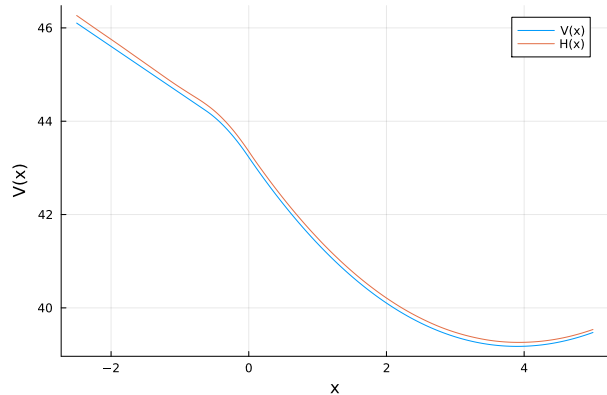
$$J(x, u) = \mathbb{E}_x \left[\int_0^\infty e^{-rt} f(X(t)) dt + \sum_j e^{-r\tau_j} c(y_j) \right], \quad (39)$$

where the cost functions $f(\cdot)$ and $c(\cdot)$ are as defined in Section 3.

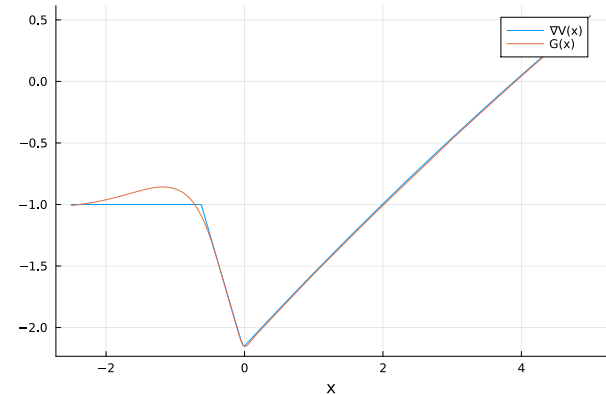
The problem parameters for the one-dimensional test problem are listed in Table 14. The hyper-parameter configuration for this example was determined empirically. The terminal time is $T = 0.8$, and the number of time intervals is $N = 200$. The batch size is $K = 1250$. For the neural-network architecture, the hidden layers have width 250, and we use four hidden layers with ELU activation functions in this one-dimensional example. During training, we use learning rates 10^{-3} , 10^{-4} , and 10^{-5} consecutively, each for 5000 iterations, to achieve high accuracy. The penalties are 10^2 , 10^4 , and $2 \cdot 10^5$, also for 5000 iterations each, and the cost scaling parameter is set to $\kappa = 1.0$ (no scaling). The primitives of the reference policy are $\lambda = 0.4$ and Φ is lognormal with mean 2.0 and variance 1.0. Figure 3 shows that the neural-network approximations determined via our numerical procedure are close to the exact solutions for the optimal value function and its derivative in the one-dimensional setting.

Table 14: Problem parameters for one-dimensional example with diffusion demand

r	p	h	c	c_0	μ	σ
0.05	2	0.5	1	1.5	1	0.2



(a) $V(x)$ and $H_\theta(x)$



(b) $\nabla V(x)$ and $G_\vartheta(x)$

Figure 3: Value function and gradient computed using the expressions in Sulem (1986), and the neural network approximations